SYNTHESIS OF 2-FLUORO-2-DEOXY-β-D-ALLOSE, A POTENTIAL PET TRACER

Dedicated to my parents and my wife, Shaima

ELECTROPHILIC FLUORINATION OF 3,4,6-TRI-*O*-ACETYL-D-GLUCAL IN ANHYDROUS HYDROGEN FLUORIDE: SYNTHESIS OF 2-FLUORO-2-DEOXY-β-D-ALLOSE, A POTENTIAL PET RADIOTRACER FOR BREAST TUMOUR

By

REZWAN ASHIQUE, B.Sc.

A Thesis

Submitted to the School of Graduate Studies

in Partial Fulfilment of the Requirements

for the Degree

Master of Science

McMaster University

MASTER OF SCIENCE (2005) **McMaster University**

(Chemistry) Hamilton, Ontario

TITLE: Electrophilic Fluorination of 3,4,6-tri-*O*-acetyl-D-glucal in Anhydrous Hydrogen Fluoride: Synthesis of 2-fluoro-2-deoxy-β-D-allose, A Potential PET Radiotracer for Breast Tumour

AUTHOR: Rezwan Ashique, B.Sc. (McMaster University)

SUPERVISOR: Professor R. V. Chirakal and Professor G. J. Schrobilgen

NUMBER OF PAGES: xiv, 78

Abstract

In light of the increasing interest in the syntheses of fluorocarbohydrates as well as in their radiolabelled analogues for use in positron emission tomography (PET), a two-step synthesis of 2-fluoro-2-deoxy-β-D-allose (2-FDβA) has been developed. The present synthesis employed electrophilic fluorination of 3,4,6-tri-*O*-acetyl-D-glucal in anhydrous HF (aHF) solvent using F_2 and AcOF and was more rapid and efficient than the existing synthesis of 2-deoxy-2-fluoro-D-allose, with a total synthesis time of approximately 45 min, and less laborious. The synthesis proved to be higly regio- and stereosective, which is often hard to achieve from electrophilic fluorinations.

The synthetic route to 2-FDβA was used to obtain the ^{18}F-labelled analogue, 2-[^{18}F]FDβA, for the first time with the anticipation that the labelled compound will be of use as a diagnostic agent for the detection and assessment of different tumours as well as for monitoring D-allose metabolism. The overall decay-corrected radiochemical yields (RCY) of the products resulting from radiofluorination of TAG in aHF with [^{18}F]F_2 and [^{18}F]AcOF were 33 ±3% and 9 ±2%, respectively, with respect to [^{18}F]F_2. The RCY of 33 ±3% is the highest reported for direct fluorinations of TAG using [^{18}F]F_2 in any solvent. The radiochemical purities of 2-[^{18}F]FDβA were 96 ±3% and 91 ±8% as determined by radio-HPLC and radio-TLC, respectively. Preliminary *in vivo* studies using normal rats showed significant differences between the uptake of 2-[^{18}F]FDβA and 2-[^{18}F]FDG, the most commonly used PET radiotracer for detection of various types of cancers. In addition, an animal study with a Polynoma Middle T mouse showed retention of 2-[^{18}F]FDβA in the tumour. The ^{18}F-labelling technique was also used as a mechanistic probe for the synthesis of 2-FDβA in the present study.

Acknowledgements

I most sincerely would like to thank my supervisors, Dr. Raman V. Chirakal and Dr. Gary J. Schrobilgen. I am grateful to Dr. Schrobilgen for his continued support and guidance and for always making time for me even on his busiest and most hectic day. I also very much appreciate the financial support provided by Dr. Schrobilgen. There are no words that could express my gratitude towards Dr. Chirakal. From the very first day that I passed through his lab door, he treated me more like a colleague than just a student. I thank him for his outstanding supervision and patience and especially for putting up with me. I also thank both Dr. Chirakal and Dr. Schrobilgen for sharing their knowledge and expertise to successfully complete the research.

I wish to express thanks to Dr. Hélène P. A. Mercier for all her help and advice throughout the course of my research. I would also like to thank Dr. Paul Harrison for his interest in my research and helpful suggestions.

I would like to take this opportunity to show my appreciation to Dr. Karen Gulenchyn, the Chief of Nuclear Medicine at Hamilton Health Sciences for making the hospital facilities available for this research.

Special thanks are extended to Dr. Donald W. Hughes for the remarkable assistance with the NMR experiments as well as for his help with the interpretation of the NMR spectra. I also thank Dr. Kirk Green for his help with acquiring the mass spectra.

I would like to acknowledge all the assistance that I have received from the wonderful ladies in both Nuclear Medicine Department and Department of Chemistry office, with special thanks to Diane David (Nucl. Med.) and Carol Dada (Chem.).

I wish to thank Dr. Troy Farncombe, Dr. Renée Labiris and Chantal Saab for their help with the *in vivo* studies. I also thank Dr. Farncombe for always sparing his time to provide me with details on anything to do with PET.

I thank all my past and present colleagues in both Nuclear Medicine Department and Dr. Schrobilgen's lab group for the great times and for turning any given stressful day into a relaxed one. Special thanks go to Babak Behnam Azad for making the working days in the past few months really enjoyable.

Hearty gratitude must be shown to all the friends that I have made along the way at McMaster, especially Ramana, Hark, Greg B., Greg S., Tina, Adam, Matt P. and Richard. Their valued friendship and support have made this journey very pleasant and memorable one. I am also grateful to my dearest friends, Nafis and Raju, for their friendship that have lasted for so many years and for all their help with my personal life.

The most difficult job is to acknowledge two people - Shaima Anam and Dr. Neil Vasdev. I wish to show my gratitude to Shaima, my wife, for her everlasting patience and unlimited belief in me and especially for her untiring support and understanding in the past few months. I gratefully thank Neil most importantly for his brotherly friendship over the past few years. I also thank him for his continuing help, advice and suggestions with both my research and career. Honestly speaking, if not for Shaima, Neil and Dr. Chirakal, I would never be where I am now.

Above all, I thank my parents for their immense and unselfish love, support and encouragement throughout my life.

TABLE OF CONTENTS

LIST OF FIGURES

LIST OF TABLES

LIST OF ABBREVIATIONS AND SYMBOLS

General

aHF	anhydrous hydrogen fluoride
i.d.	inner diameter
kJ	kilojoules
o.d.	outer diameter
ACN	acetonitrile
ESI	electrospray ionization
FDG	2-fluoro-2-deoxy-D-glucose
FDβA	2-fluoro-2-deoxy-D-allose
FDM	2-fluoro-2-deoxy-D-mannose
FEP	perfluoroethylene/perfluoropropylene copolymer
Kel-F	chlorotrifluoroethylene polymer
HPLC	high performance liquid chromatography
MS	mass spectrometry
Teflon (PTFE)	tetrafluoroethylene polymer
TLC	thin layer chromatography

Nuclear Magnetic Resonance

δ	chemical shift
J	nuclear spin-spin coupling constant
ppm	parts per million
FID	free induction decay

COSY	correlation spectroscopy
HSQC	heteronuclear single quantum coherence
MLEV	
SF	spectrometer frequency
SW	spectral width
TMS	trimetylsilylchloride
TOCSY	total correlation spectroscopy

Radiochemistry

α	alpha
β^+	postiron
β^-	beta particle
d	deuteron
γ	gamma
keV	kiloelectron volts
λ	decay constant
n	neutron
n.c.a.	no-carrier-added
p	proton
t	triton
$t_{1/2}$	half-life
ν	neutrino
A_o	radioactivity at zero time

A_t	radioactivity at time t
Ci	curie
MeV	megaelectron volts
MRI	magnetic resonance imaging
PET	positron emission tomography
RCY	radiochemical yield
SPECT	single photon emission computed tomography

CHAPTER 1

INTRODUCTION

1.1 Fluorine

Fluorine is monoisotope in nature. Because of its extreme reactivity, fluorine does not occur as F_2 in nature and is mostly found as F^- ion in minerals such as cryolite, fluorite and apatite.[1] From the time of the discovery of fluoride in 1771 by Karl Wilhelm Scheele,[2] attempts to obtain F_2 from its compounds were frequently made. Although the first real attempts to obtain F_2 were made by Sir Humphry Davy[3] between the years 1811-1813, Henri Moissan[4,5,6] was the first to successfully isolate F_2 gas in 1886. Moissan prepared F_2 gas by electrolysis of anhydrous hydrogen fluoride in the presence of potassium fluoride.

Fluorine, in its compounds, is the most electronegative element in the Periodic Table (4.0 on the Pauling scale of electronegativity[7]) and as the element, F_2, it is the most reactive. The fluorine atom is relatively small and the ionic radius of fluoride ion is the smallest of any known monovalent anion (ionic radius, 1.33 Å[8]). Fluorine bonds with row 2 elements are very short and strong,[9] for example, with typical C–F bond length of 1.32 Å and a mean theoretical C–F bond energy in CF_4 of 546.0 kJ mol^{-1}, which is 99.6 kJ mol^{-1} higher than the C–H bond energy in CH_4 (446.4 kJ mol^{-1}).[10]

1.2 Organofluorine Chemistry

Organofluorine chemistry began with Schmitt[11] in 1870 when he synthesized the first compound containing an aryl C–F bond. Subsequent direct fluorination of organic substrates with F_2 were often shown to be highly unselective and extremely exothermic owing to the high heats of formation of C–F (ca. -430.5 kJ mol^{-1})[12] and H–F

(-273.3 kJ mol^{-1})[13] bonds. The high reactivity of fluorine towards organic substrates is also the result of the relatively low bond dissociation energy (BDE) of fluorine-fluorine bond (157.7 kJ mol^{-1}), compared with the BDEs of the carbon-fluorine bonds (452-531 kJ mol^{-1}),[14] which can be readily formed by reaction of elemental fluorine with hydrocarbons.[15] Hence, the latter fluorination process most likely proceeds by a radical chain mechanism (Table 1.1).[12] The heat dissipated during such a fluorination reaction, in the absence of a thermal sink, such as $CFCl_3$ solvent, is high enough to result in the destruction/oxidation of the molecule, often leading to the production of tars and occasional explosions. As a result, many direct fluorination methods that use elemental fluorine for the introduction of fluorine into organic substrates, such as LaMar process, aerosol fluorination and fluorination using microreactors,[10] and approaches using other fluorinating agents have been developed that pose significant ongoing synthetic opportunities and challenges in modern fluorine chemistry.

Table 1.1. Thermodynamic Data for the Fluorination of Methane.[12]

			ΔH° (kJ mol^{-1})	
Initiation				
F_2	→	2F·	157.7	(1.1a)
R-H + F_2	→	R· + HF + F·	16.3	(1.1b)
Propagation				
R-H + F·	→	R· + HF	-141.4	(1.2a)
R· + F_2	→	R-F + F·	-289.1	(1.2b)
Termination				
R· + F·	→	R-F	-446.8	(1.3a)
R· + R·	→	R-R	-350.6	(1.3b)
Overall Reaction				
R-H + F_2	→	R-F + HF	-430.5	(1.4)

1.3 Medical Applications of Fluorine

The substitution of fluorine in biologically active molecules has a long and successful history and is presently widely applied.[16] Elemental fluorine is in many ways unique in chemical characteristics as well as in its usefulness in the pharmaceutical and chemical industries. The selective fluorination of biomolecules has had a long and successful history in medicinal chemistry.[14,17] Substitution of fluorine for hydrogen in biologically active molecules is not expected to produce a large steric perturbation because the van der Waals radius of the fluorine atom (1.47 Å)[10] is similar to that of hydrogen (1.20 Å),[10] and the C–F bond length (1.26 – 1.41 Å) is not much greater than the C–H bond length (1.08 – 1.11 Å).[18] However, because fluorine is highly electronegative and carbon-fluorine bond energies are very high, substitution of fluorine in biomolecules can often produce significant and useful changes in physiochemical and biological properties of such molecules.[16] In some cases, fluorine substitution produces a derivative with improved pharmacological properties. For example, replacement of hydrogen by fluorine usually increases lipid solubility, thus enhancing the rate of *in vivo* absorption and transport of labelled compounds.[19] Although fluorine is generally considered as an isosteric replacement for hydrogen, it is also an isostere for oxygen (van der Waals radius: 1.52 Å; C–O bond length: 1.43 Å).[20] The differences in electronegativity (4.0 for fluorine compared with 3.5 for oxygen[7]) and the hydrogen bonding capability of fluorine often allow it to mimic a hydroxyl group.[16]

Overall, introduction of fluorine into biomolecules can be used to block metabolism, to function as a leaving group in enzyme inhibition, to function as a probe of hydrogen bonding or as a potent substituent for modifying the chemical reactivity of an

adjacent functional group.[19] The extensive chemistry of the stable isotope of fluorine, ^{19}F, in biomolecules has made possible the use of biologically active molecules labelled with the radioactive isotope of fluorine, ^{18}F, for medical imaging purposes.

1.4 Isotopes of Fluorine

The only stable isotope of fluorine is ^{19}F, which is 100% naturally abundant. Although naturally occurring fluorine is monoisotopic, there are eight man-made radioactive isotopes of fluorine (Table 1.2)[20] that have been produced since the 1930's. Fluorine-17 and ^{18}F are neutron deficient, i.e., they have a neutron to proton ratio less than that of ^{19}F and decay by positron (β^+) emission. The positron is a positively charged anti-particle of an electron, which is emitted from the nucleus of a radioactive isotope. The other six radioactive isotopes of fluorine are neutron rich, that is, they have a neutron to proton ratio greater than that of the stable nuclide and decay by negative beta (β^-) emission.

Table 1.2. Isotopes of fluorine.[20]

Isotope	Half-life	Decay Mode	Product
^{17}F	64.5 s	β^+	^{17}O
^{18}F	109.7 min	β^+	^{18}O
^{19}F	stable		
^{20}F	11.0 s	β^-	^{20}Ne
^{21}F	4.4 s	β^-	^{21}Ne
^{22}F	4.1 s	β^-	^{22}Ne
^{23}F	2.2 s	β^-	^{23}Ne
^{24}F	0.34 s	β^-	^{24}Ne
^{25}F	59 ms	β^-	^{25}Ne

1.5 Radiochemistry

Radiochemistry is concerned, in all its aspects and objectives, with radioactivity, using nuclear phenomena for the investigation of chemical properties and reactivity. The birth of radiochemistry dates from the discovery of polonium and radium in trace amounts, at a period just following the recognition of natural radioactivity. In its advance and extension, the new discipline progressively attained an individual character within nuclear science and later became a subtopic of chemistry, contributing to the subsequent discoveries of artificial radioactivity, fission and the transuranium elements. Although chemistry has played an important role in nuclear science, radiochemistry, in turn, has contributed to the development of several branches of chemistry. Yet, in the course of its evolution as a discipline, radiochemistry has frequently been involved in numerous research subjects and scientific fields outside of chemistry, such as medical imaging in nuclear medicine. At present, it is clear that radiochemistry is, by nature, a field that employs radioisotopes to study the properties of the stable isotope at infinite dilution.[21]

1.6 Nucleonics

Radioisotopes or radionuclides are isotopes of an element that possess nuclei that are unstable in their ground states. A radionuclide tries to attain stability by emitting electromagnetic radiation or charged particles through a process called radioactive decay. Stability may be achieved either by direct (single-step) decay to a stable nuclide or by decay to several radionuclides in multiple steps and, finally, to a stable nuclide. There are three radioactive decay processes, alpha (α), beta (β) and gamma (γ) emission. Radionuclides undergoing β-decay may attain stability through β^- (or electron) emission, β^+ emission or electron capture.[22]

The nature of the decay, in conjunction with the emitted energy and half-life, determine the potential applications of a radionuclide. For example, radionuclides that decay by γ or β^+ emission are most suited for imaging, while radionuclides that decay by β^- and α emission and by electron capture are potentially more useful for therapeutic applications.

In the present research, only β^+ decay is considered. As stated earlier, a positron is an electron with a unit positive instead of a unit negative charge. Thus, it has the same mass as an electron.[22] Positron decay occurs for radionuclides that are neutron deficient or proton rich. In such decay processes, a proton (p) transforms into a neutron (n) by emission of a β^+ particle and a neutrino (ν), which is an entity almost without mass and charge and is primarily needed to conserve energy in the decay process (eq. 1.5).[23]

$$p \rightarrow n + \beta^+ + \nu \tag{1.5}$$

Positron emission takes place when the energy difference between the parent and daughter nuclides is greater than 1.02 MeV.[23] Because a β^+ particle can be emitted with an energy between zero and the decay energy, the neutrino carries away the difference between the decay energy and β^+ energy. After β^+ decay, the daughter nuclide has an atomic number that is 1 less than that of the parent (eq. 1.6).[22]

$$^{A}_{Z}X \longrightarrow {}^{A}_{Z-1}Y + \beta^+ + \nu \tag{1.6}$$

Some examples of β^+ decay follows:[22]

$$^{15}_{8}O \longrightarrow {}^{15}_{7}N + \beta^+ + \nu \tag{1.7}$$

$$^{18}_{9}F \longrightarrow {}^{18}_{8}O + \beta^+ + \nu \tag{1.8}$$

$$^{52}_{26}Fe \longrightarrow {}^{52}_{25}Mn + \beta^+ + \nu \tag{1.9}$$

1.7 Radiopharmaceuticals and Radiotracers

A tracer is an element or compound introduced into a biological system to determine the distribution and/or metabolism of materials. Moreover, a tracer should not affect the process it is used to measure.[24] In the context of this Thesis, radiotracers are biologically active compounds labelled with a radionuclide, which are prepared in a form suitable for *in vivo* administration for diagnostic or therapeutic purposes. Radiotracers that are free from all toxic impurities as well as unwanted radionuclides, appropriately sterilized and carefully formulated and certified to be safe for *in vivo* use, are referred to as radiopharmaceuticals. The biomolecule in a radiopharmaceutical determines its biodistribution, while the radionuclide, upon its decay, serves as the tag that is used to monitor the biochemical process under study. Unlike conventional drugs, radiopharmaceuticals are usually administered in trace quantities in a single dose and, hence, produce no pharmacologic effects.[23] Because certain biomolecules are specifically retained in a particular organ, a radiopharmaceutical can be used to probe the function of the organ in a non-invasive way. As a result, radiopharmaceuticals are widely used to obtain diagnostic information of target tissues on organs, such as the location of cancerous growths or obstructions of blood flow in a patient or to provide therapeutic results.[25]

1.8 Nuclear Medicine

Nuclear medicine is a specialized subset of radiology and a vital medical specialty that involves radiopharmaceuticals for diagnosis, management, treatment and prevention of serious diseases. Nearly 95% of the radiopharmaceuticals employed in nuclear medicine are used for diagnostic purposes, while the remainder are used for therapeutic

treatments.[23] The origin of nuclear medicine stems from many scientific discoveries, most notable is the discovery of X-rays in 1895 and the invention of the cyclotron by Ernest Orlando Lawrence in the mid 1930's which resulted in the discovery of artificial radioactivity. A landmark event for nuclear medicine, which has often been considered as the true beginning of nuclear medicine, occurred in 1946 when the treatment of a thyroid cancer patient with radioactive iodine (^{131}I) resulted in the complete eradication of the metastasis associated with the patient's cancer. Nuclear medical imaging is unique in that it documents organ function and structure, in contrast with diagnostic radiology, which is based upon anatomy. Nuclear medicine procedures often detect abnormalities very early in the progression of a disease, allowing for a disease to be treated early in its development, resulting in a more successful prognosis. Today there are approximately 100 different nuclear medicine imaging procedures that provide information about nearly every organ system.

1.9 Positron Emission Tomography: An Imaging Technique in Nuclear Medicine

Positron emission tomography (PET) is a nuclear medicine imaging technique that employs the concepts of computerized tomography in conjunction with physiologically active compounds labelled with β^+ emitting radionuclides to image and measure the function of *in vivo* biological processes with minimal disturbance.[26] A positron emission tomograph permits the accurate quantification of the distribution of radioactivity in the body and allows for the study of physiology, molecular biology, energy metabolism, drug-receptor or drug-enzyme interactions and the *in vivo* fates of radiopharmaceuticals.[27] Medical imaging with PET examines the biological origin of a disease so that illness may be diagnosed and treated at an early stage and more

effectively. Whole-body PET imaging guides physicians to the most appropriate treatment for the disease to which it is applied. For example, whole-body PET imaging with 2-[^{18}F]fluoro-2-deoxy-D-glucose (2-[^{18}F]FDG), by far the most commonly used radiotracer for PET studies, enables inspection of glucose metabolism in all organ systems in a single examination and provides improved detection and staging of cancer, selection of therapy, and assessment of therapeutic response.[26] It has been shown that PET is complementary to conventional X-ray, single photon emission computed tomography (SPECT), and magnetic resonance imaging (MRI) techniques.[28,29]

After radiopharmaceuticals labelled with β^+ emitting radionuclides are introduced into the body, the β^+ emitted from the radionuclide travels several millimetres within the tissue, during which time it loses its kinetic energy through ionization and excitation interactions. Once a β^+ has lost sufficient energy, it will undergo an annihilation reaction with its anti-matter particle, the electron, resulting in the creation of two energetic, body-penetrating annihilation photons (gamma rays). The annihilation photons have energies of 511 keV each and are emitted at approximately 180° to each other. Individual positron decay events are localized by two coincidence detectors mounted at 180° to each other. The coincident detection of the annihilation photons by an array of detectors or scintillation counters, usually placed along the circumference of a circle, enables the determination of the line along which the annihilation event occurred.[30] A projection of the distribution of the activity is obtained by rotating the coincidence line over the section to be measured. The projections recorded at various angles between 0 and 180° provide a spatial image of the distribution of the β^+ emitter with a horizontal resolution of 4 to 6 mm and slice thickness of 8 to 10 mm. The detector signals are represented as

tomographic images that reveal the spatial distribution of the radioactivity.[21] Consequently, one of the advantages of PET is that it allows the absolute measurement of isotope concentration in tissue, permitting quantitative assessment of physiological parameters.[31] As an example, the positron decay and detection of ^{18}F by PET is shown in Figure 1.2.

1.10 Criteria for the Production of PET Radiopharmaceuticals

In PET, or nuclear medicine in general, radionuclides are rarely used in their simplest chemical form such as $^{18}F^-$ ion. Instead, they are incorporated into a variety of biologically active compounds referred to as radiotracers or radiopharmaceuticals, as described earlier. The PET data are strongly dependent upon the radiopharmaceuticals employed. Several criteria must be considered in the development of synthetic routes to short-lived PET radiopharmaceuticals.

Because a radiopharmaceutical consists of a biomolecule and a radionuclide, two considerations apply in designing or developing radiopharmaceuticals, one relating to the biomolecule and the other relating to the radionuclide. Besides being non-toxic in the desired amount, important factors affecting the selection of the biomolecule are the biodistribution of the molecule of interest, its selectivity and blood brain permeability as well as its type of binding in the target organ or tissue.[20] The latter is generally expressed as target to non-target ratio. In order to obtain a higher contrast in the image, which aids in visualizing a disease with ease, the target to non-target ratio must be high. Three important variants that determine or affect the distribution and localization of a biochemical in the target organ are route of administration, blood flow to the organ or

Figure 1.1. The positron decay and detection of ^{18}F by the use of PET.

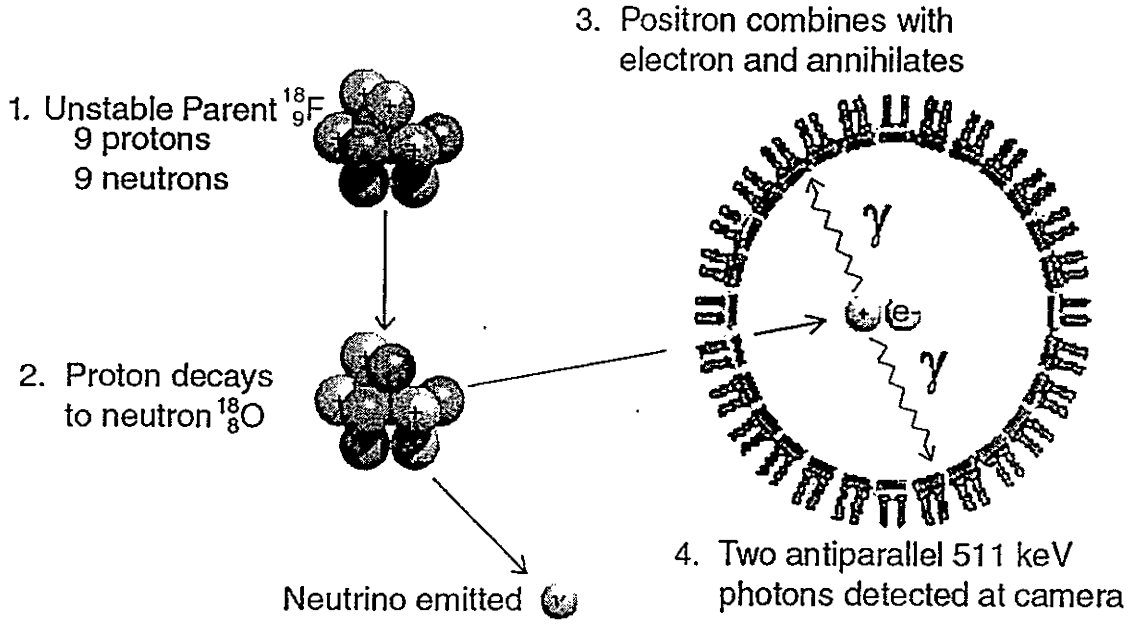
3. Positron combines with electron and annihilates
1. Unstable Parent $^{18}_{9}F$
9 protons
9 neutrons
2. Proton decays to neutron $^{18}_{8}O$
Neutrino emitted
γ
e
γ
4. Two antiparallel 511 keV photons detected at camera

tissues and extraction (of the biochemical) by the tissues. The choice of radionuclide for imaging purposes is primarily directed by the constraint of minimizing the radiation dose to the patient and by the detection characteristics of the instrumentation presently used in nuclear medicine. To minimize the radiation dose to the patient, it is suggested that the half-life of the radionuclide should be about $ln2 \times T_{obs}$, where T_{obs} is the time interval between the time of administration of radionuclide and the time at which measurement or scanning is performed.[22]

Once a particular labelled compound has been established for *in vivo* use with PET, several aspects must be taken into consideration including the radiochemical yield (RCY), specific activity, total synthesis time and reproducibility from the synthetic standpoint as well as the radionuclidic, radiochemical and chemical purities, shelf-life, sterility and apyrogenicity from the quality control standpoint.

The RCY is the most important criterion for the development of radiopharmaceuticals for routine clinical use in PET, because any method used for radiolabelling must provide sufficient quantities of the labelled product at the end of the synthesis. The RCY is the percent of radionuclide incorporated into the radiopharmaceutical in its desired form. The RCY indicates the efficiency of a radiochemical synthesis. However, a high yield synthesis may not be practical for the development of a radiopharmaceutical for *in vivo* PET studies if the synthesis time is too long.[32]

Specific activity is the amount of radioactivity per unit mass of the labelled compound. The specific activity of the labelled molecule should be as high as possible for it to behave like a tracer. A radiochemical synthesis resulting in a radiolabelled

compound having a high RCY and purity, yet low specific activity, is usually not desirable for developing PET radiopharmaceuticals.[32]

It is ideal and desirable to synthesize radiopharmaceuticals for routine use. As a result, radiochemical syntheses, that ensure reproducibility of yield and purity, must be devised. The method for the production of the radionuclide affects the radionuclidic purity of a radiopharmaceutical, which is a measure of the amounts of other radionuclides contained in the final product. Ideally, a radiopharmaceutical should contain only the desired radionuclide, however, it is often not possible to avoid some minimal contamination by other radionuclides.[22]

Because a radionuclide may occur in several compounds, it is important to make sure that a given radiopharmaceutical is in the desired chemical form.[22] Radiochemical purity is defined as the fraction of a specific radionuclide incorporated into the desired molecule. In the case of ^{18}F, radiochemical purity is expressed as the percentage of the total ^{18}F in the final product that is in the desired form.

Similarly, enantiomeric purity of a radiopharmaceutical often influences its biological activity. It is customary to separate racemic mixtures having different biological activities so that the undesirable enantiomer does not increase the radiation dose to the patient or degrade the image quality by increasing background levels of radiation.[22,32]

During the synthesis of a radiopharmaceutical, it is possible to have a number of compounds involved besides the radiochemical of interest. If these compounds cannot be eliminated, they should be safe for the patient. Moreover, these additional compounds must not influence the *in vivo* function of the main compound. However, for an ideal

radiopharmaceutical, the chemical purity should be optimized by characterizing as many of the by products as possible so that the amounts of undesirable by products can be minimized or eliminated.[22]

The shelf life of a radiopharmaceutical is the time during which it can be used effectively. With a short-lived radiopharmaceutical, the half-life determines the shelf-life, providing that the decomposition and/or contamination level is zero or very low over the same time period.[33]

When a radiopharmaceutical is administered, it must be sterile, i.e., free from any microbial contamination, as well as free from pyrogens, substances that cause fever. The radiopharmaceutical should be tested for these effects prior to administration to the body. However, where prior testing is not always feasible, the sterility and apyrogenicity of the labelling technique should be properly ascertained as a periodic basis.[22]

1.11 Positron Emitting Radionuclides in PET

Several factors must be considered in the selection of the β^+ emitting radionuclide for the design and syntheses of radiopharmaceuticals for PET studies. *In vivo* PET is mostly based upon the use of four radionuclides, namely, ^{11}C, ^{13}N, ^{15}O, and ^{18}F (Table 1.3). The reason why these nuclides are so commonly used is that they can be readily substituted directly into biomolecules. Moreover, ^{11}C, ^{13}N and ^{15}O are often referred to as the radioisotopes of the "elements of life". Substitution of ^{11}C does not significantly alter the reaction time or mechanisms of a molecule. A similar situation exists for ^{13}N and ^{15}O. Fluorine-18 can often be substituted for hydrogen or a hydroxyl group of a biomolecule or placed in a position where its presence does not significantly alter the biological behaviour of the molecule.[16] The short half-lives of the four above-

mentioned radionuclides serve to reduce doses to tissues. The 511 keV photons resulting from the annihilation of positrons emitted from these radionuclides with their antiparticles allow the *in vivo* physiological processes occurring to be quantified by detectors outside the body. Despite the advantages discussed above, the relatively short half-lives of ^{11}C, ^{13}N and ^{15}O generally limit their use to studies requiring measurements lasting less than an hour. On the other hand, ^{18}F with its longer half-life has proven to be the most practical and useful β^+ emitter for PET studies.

Table 1.3. Characteristics of Positron Emitters Used in PET Studies.[16,20,21,32]

Nuclide	Half-life (min)	Common Method of Production	Max. Energy (MeV)	Max. Range[i] (mm)	Max. Theoretical Specific Acitivity (Ci/mole)
^{11}C	20.4	$^{14}N(p,\alpha)^{11}C$ $^{11}B(p,n)^{11}C$	0.96	4.11	9.22×10^9
^{13}N	9.96	$^{12}C(d,n)^{13}N$ $^{13}C(p,n)^{13}N$ $^{16}O(p,\alpha)^{13}N$	1.19	5.4	1.89×10^{10}
^{15}O	2.07	$^{14}N(d,n)^{15}O$ $^{15}N(p,n)^{15}O$	1.70	8.0	9.08×10^{10}
^{18}F	109.7	$^{20}Ne(d,\alpha)^{18}F$ $^{18}O(p,n)^{18}F$	0.635	2.4	1.71×10^9

[i]In water

1.12 Advantages of the Use of Fluorine-18 in PET Studies

Among the rationales for the extensive use of ^{18}F in PET studies are the properties of the element and the nuclear properties of the isotope. The elemental properties and the medical applications of fluorine have already been discussed in earlier sections. When

replacing ^{19}F in a biomolecule with a radioactive isotope of fluorine, the radiotracer has essentially the same properties as the unlabelled compound and the small isotopic effect may be regarded as negligible.[34]

Among the eight known radioisotopes of fluorine, ^{18}F has the longest half-life (109.7 min), however, its production and subsequent experimental work with it should be carried out within two half-lives.[35] Although the half-life of ^{18}F is relatively short from the point of view of a synthetic chemist, there are several advantages associated with this isotope. The short half-life of ^{18}F reduces problems with storing and handling of radioactive waste. Furthermore, the short half-life and easy detection of the 511 keV gamma-rays from the annihilation of its positron decay, along with the high C-F bond dissociation energy of 485 kJ mol^{-1},[14] make ^{18}F-labelled compounds ideal as radiotracers.

The half-life of ^{18}F is significantly longer when compared with the positron emitting isotopes of carbon, nitrogen and oxygen (Table 1.3). This permits sufficient time for the syntheses of ^{18}F-labelled compounds and for performing quality control prior to patient injection, as well as adequate time for the labelled compound to accumulate in tissues while limiting radiation exposure to the patient. The positron energy of ^{18}F is only 0.635 MeV, resulting in low radiation doses and good image quality. Another advantage of ^{18}F is that its 109.7 min half-life makes it possible to transport ^{18}F-labelled compounds to satellite facilities and hospitals that do not possess on-site cyclotron facilities.[36] Figure 1.2 shows some examples of ^{18}F-labelled radiopharmaceuticals that are used in routine clinical PET studies.

1.13 Production and Recovery of Fluorine-18

Fluorine-18 can be produced for clinical and medical purposes by a number of a

Figure 1.2. Examples of ^{18}F-labelled radiopharmaceuticals used in PET studies.

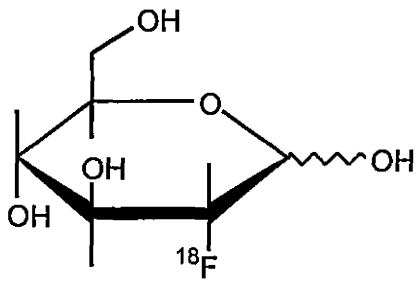

2-[^{18}F]Fluoro-2-deoxy-D-Glucose
(2-[^{18}F]FDG)

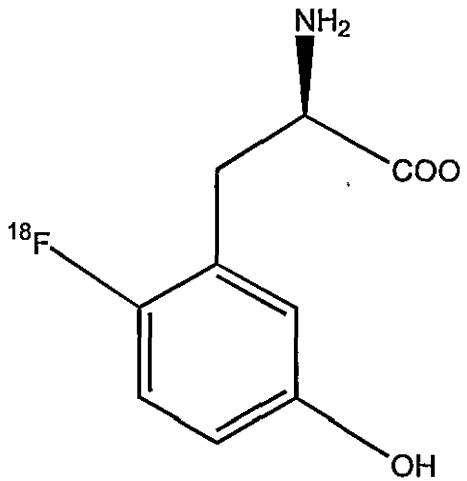

6-[^{18}F]Fluoro-L-*m*-tyrosine
(6-[^{18}F]FMT)

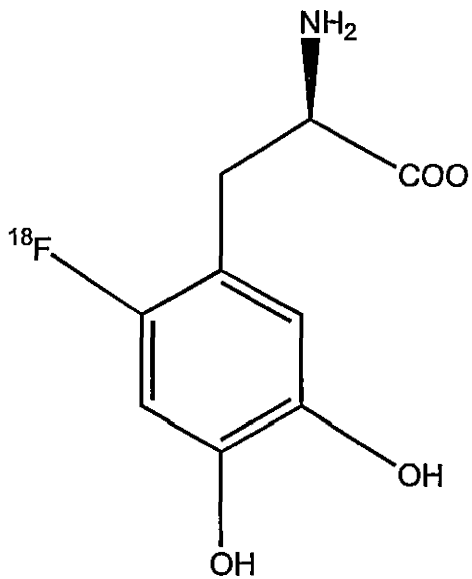

6-[^{18}F]Fluoro-L-DOPA
(6-[^{18}F]FDOPA)

nuclear reactions,[9] however, in all cases a fast neutron source, accelerator, cyclotron or nuclear reactor is required. Depending on the method used, either electrophilic ($[^{18}F]F_2$) or nucleophilic ($^{18}F^-$, $[^{18}F]HF$) species can be produced. Methods for the production of ^{18}F are listed in Table 1.4.

Prior to 1983, ^{18}F was produced at McMaster University by the use of a nuclear reactor, requiring a rather complicated two-step process involving fast neutron bombardment of a solid lithium-6 target to generate the requisite tritons to drive the $^{18}O(t,n)^{18}F$ reaction (Table 1.4, Method 1). This method never resulted in a practical approach because the ^{18}F produced was contaminated with radioactive tritium resulting from the initial nuclear reaction, $^{6}Li(n,\alpha)^{3}H$. At present, methods for ^{18}F production involving the use of a cyclotron are clearly the preferred choice owing to the greater simplicity of the target designs, as well as the overall higher yields of the radionuclide.[16] The most common nuclear reactions used to produce ^{18}F are $^{18}O(p,n)^{18}F$ (Table 1.4, Methods 8-11) and $^{20}Ne(d,\alpha)^{18}F$ (Table 1.4, Method 14). The former has been shown to be more efficient than the latter,[37,38] because the proton bombardment of enriched ^{18}O provides significantly higher yields and specific activity.[38] In addition, the relatively wide availability of proton cyclotrons, which use moderate beam energies and currents to provide useful yields[33] make the $^{18}O(p,n)^{18}F$ nuclear reaction more widely accessible than the $^{20}Ne(d,\alpha)^{18}F$ nuclear reaction.

The $^{18}O(p,n)^{18}F$ reaction is convenient for use with a proton-only cyclotron and is mainly used for the production of $[^{18}F]F_2$ and ^{18}F-fluoride ($^{18}F^-$) by irradiation of enriched $^{18}O_2$ and $H_2{}^{18}O$, respectively (Table 1.4, Methods 8,10,11). The ^{18}F activity is recovered

Table 1.4. Methods for the Production of Fluorine-18.

Method	Source[i]	Nuclear Reaction	Target Material	Fluorinating Agent	Reference
1	1	$^{16}O(t^{ii},n)^{18}F$	$^{6}Li_2CO_3$	$H^{18}F$	39
2	2	$^{16}O(\alpha,2n)^{18}Ne \rightarrow {}^{18}F^{iii}$	O_2	$[^{18}F]HF$	40,41
3	2	$^{16}O(^{3}He,n)^{18}Ne \rightarrow {}^{18}F^{iii}$	O_2	$[^{18}F]HF$	40,41
4	2	$^{16}O(\alpha,d)^{18}F$	$H_2O_{(aq)}$	$^{18}F^-$	42
5	2	$^{16}O(\alpha,pn)^{18}F$	$H_2O_{(aq)}$	$^{18}F^-$	42
6	2	$^{16}O(^{3}He,p)^{18}F$	$H_2O_{(aq)}$	$^{18}F^-$	43
7	2	$^{16}O(^{3}He,p)^{18}F$	O_2	$[^{18}F]F_2$	44
8	2	$^{18}O(p,n)^{18}F$	$^{18}O_2$	$[^{18}F]F_2$	38,45
9	2	$^{18}O(p,n)^{18}F$	$CO^{18}O_{(s)}$	$^{18}F^-$	46
10	2	$^{18}O(p,n)^{18}F$	$H_2{}^{18}O_{(s)}$	$^{18}F^-$	47
11	2	$^{18}O(p,n)^{18}F$	$H_2{}^{18}O_{(aq)}$	$^{18}F^-$	48
12	1	$^{19}F(n,2n)^{18}F$	$[NH_4]HF_2]$	$[^{18}F]HF$	49
13	2	$^{20}Ne(p,2pn)^{18}F$	Ne	$[^{18}F]F_2$	50
14	2,3	$^{20}Ne(d,\alpha)^{18}F$	Ne	$[^{18}F]F_2, H^{18}F, {}^{18}F^-$	51,52
15	2	$^{20}Ne(^{3}He,\alpha n)^{18}Ne \rightarrow {}^{18}F^{iii}$	Ne	$H^{18}F$	53,54

[i]Sources 1,2 and 3 are nuclear reactor, cyclotron and accelerator, respectively.

[ii]Tritium is produced by the $^{6}Li(n,\alpha)^{3}H$ nuclear reaction.

[iii]Conversion of ^{18}Ne ($t_{1/2}$ = 1.67 s) to ^{18}F occurs through electron capture.

as $[^{18}F]F_2$ from the target by use of carrier $^{19}F_2$ or as $^{18}F^-$ directly from the target (no-carrier-added, n.c.a), which results in higher specific activities when compared with carrier-added syntheses. All experiments described in the present work involve the use of $[^{18}F]F_2$ produced from the $^{18}O(p,n)^{18}F$ nuclear reaction with an approximate specific activity of 35 Ci/mmol[55] by the use of a Siemens 11 MeV proton-only cyclotron (RDS 112) at the Department of Nuclear Medicine, Hamilton Health Sciences. It should be noted that the theoretical maximum specific activity of ^{18}F is 1.71×10^9 Ci/mol (Table 1.3).

1.14 Radiofluorination with Fluorine-18

Although discovered as early as 1937, synthetic applications of ^{18}F lagged behind radiochemical applications of carbon-11, largely because of difficulties encountered in the fluorination of organic molecules. The majority of the radiolabelling methods involving ^{18}F have been developed or greatly improved in the last two decades. Consequently, most of the ^{18}F-labelled radiopharmaceuticals for *in vivo* use have been introduced in the last twenty years.[16]

The chemical reactions used for radiolabelling with ^{18}F fall, in broad terms, into two categories, namely electrophilic and nucleophilic reactions. This categorization is based on the use of an electrophilic form of ^{18}F, $[^{18}F]F_2$, or nucleophilic form, $^{18}F^-$. Historically, many important ^{18}F-labelled radiopharmaceuticals were initially prepared by the use of electrophilic fluorination. However, many of these radiopharmaceuticals were not ideal for *in vivo* use owing to the low RCY and specific activity. As a result, these radiopharmaceuticals were subsequently synthesized by nucleophilic fluorination that provided higher RCYs and specific activities.[16] The present work utilizes only two

electrophilic radiofluorinating reagents, namely $[^{18}F]F_2$ and ^{18}F-labelled acetyl hypofluorite ($[^{18}F]CH_3COOF$ or $[^{18}F]AcOF$), and thus, the discussion in this section will be limited to these $[^{18}F]$fluorinating reagents.

Although the term *electrophilic fluorination* was introduced by Barton and co-workers[56,57] when reacting fluoromethyl hypofluorite (CF_3OF) with organic compounds, the original electrophilic radiofluorinating agent was $[^{18}F]F_2$. Nearly all electrophilic radiofluorinating agents are derived from elemental fluorine. Therefore, from a radiochemical standpoint, the highest RCY resulting from electrophilic fluorination should be achieved when $[^{18}F]F_2$ is directly used. Because elemental fluorine is a powerful oxidizing agent and very reactive, which may cause highly exothermic reactions and can result in multiple by-products, attempts have been made to suppress the reactivity of fluorine and minimize side reactions. It was found that diluting F_2 with an inert gas can moderate and control the reactivity of the element at low temperatures.[58,59] Wolf and co-workers[51] showed that mixtures of 0.1-0.5% F_2 in neon are suitable for ^{18}F production and subsequent radiofluorinations of biomolecules. Carrying out the electrophilic fluorination in a strong acid medium has a similar effect on the reactivity of fluorine.[60,61]

The synthesis of AcOF, the first member of a new oxidative family of acyl hypofluorites, and its versatility as a mild fluorinating agent was originally reported by Rozen and co-workers.[62] They observed that elemental fluorine, which is practically insoluble in, and non-reactive with acetic acid, gave rise to AcOF in the presence of a salt such as NaF, NaOAc or $NaO(O)CCF_3$. Appleman[63] isolated and characterized AcOF, proving its existence beyond any doubt. Rozen[64] later noted that AcOF was suitable for

the syntheses of ^{18}F-labelled radiopharmaceuticals. The preparation of this important electrophilic radiofluorinating agent has been re-examined over the years mainly because it is a milder fluorinating agent when compared with $[^{18}F]F_2$ and it possesses a much greater solubility over a wide range of reaction solvents. In the original methodology, reported by Shiue and co-workers,[65] $[^{18}F]$AcOF was synthesized by reacting $[^{18}F]F_2$ slowly with a solution of aqueous ammonium hydroxide in glacial acetic acid (eq. 1.10). Preparation of this precursor was later simplified and made more reliable by the development of a gas-solid phase reaction.[66,67] The method involved passing $[^{18}F]F_2$ gas through a column containing a complex of alkali metal acetate with acetic acid (eq. 1.11).

$$CH_3COONH_4 + [^{18}F]F_2 \xrightarrow{CH_3COOH} [^{18}F]AcOF + NH_4[^{18}F]F \qquad (1.10)$$

$$KOAc(HOAc)_{1.5} + [^{18}F]F_2 \longrightarrow [^{18}F]AcOF + K[^{18}F]F{\cdot}HOAc \qquad (1.11)$$

1.15 Fluorine Effect

Substitution of fluorine into biologically active compounds affects several physico-chemical properties of the substrates and alters their biological activities.[68] Aromatic compounds with fluorine in different positions can exhibit significant differences in pharmacological properties when compared with each other and with their non-fluorinated analogues.[69] Such behaviour is referred to as the *fluorine effect*.[70] For example, among 2-, 5-, and 6-$[^{18}F]$FDOPA, only 6-$[^{18}F]$FDOPA is useful for routine clinical PET studies because it shows a very specific accumulation in the striata of the brain, whereas no evidence for substantial retention of 2- and 5-$[^{18}F]$FDOPA was obtained.[71] Similarly, only 2-$[^{18}F]$FDG, in which the configuration at C2, the carbon bearing the fluorine, is *R*, is clinically useful. In 2-$[^{18}F]$fluoro-2-deoxy-D-mannose

(2-[^{18}F]FDM), the configuration at C2 is *S*, and this is considered to be a contaminant in 2-[^{18}F]FDG preparations. Placement of fluorine in specific positions on aromatic rings or addition across a double bond is, thus, a challenging and important issue from chemical, biological and pharmaceutical perspectives.

1.16 Objectives of the Present Work

Direct fluorination reactions require that the solvent be inert to elemental fluorine and capable of dissolving both the substrate and F_2.[61] Solvents with high dielectric constants, such as strong acids, aid in polarizing the fluorinating agent. As shown in eq. (1.12), the electronegative end (X) of the electrophilic fluorinating agent is polarized by forming a hydrogen bond with the acid (HA), while the electropositive end is free to react.[60] Hence, higher electrophilic fluorination rates are expected.

$$X{-}F \xrightarrow{HA} F^{\delta+}\cdots X^{\delta-}\cdots H^{\delta+}\cdots A^{\delta-} \qquad (1.12)$$

In addition, recent studies of the electrophilic fluorinations of aromatic compounds have shown that the reactivity and regioselectivity of fluorine substitution varies significantly with the acidity of the reaction medium.[60,72,73] For example, fluorination with F_2 in anhydrous HF or HF/BF_3 has been reported to be an efficient method for the production of ^{18}F-labelled aromatic amino acids.[74,75,76]

The purpose of this study was to develop a rapid and efficient synthesis of 2-deoxy-2-fluoro-D-allose (2-fluoro-2-deoxy-D-allose) by electrophilic fluorinations of 3,4,6-tri-*O*-acetyl-D-glucal (TAG), the most common precursor used for synthesizing 2-deoxy-2-fluoro sugars by electrophilic fluorinations, in anhydrous hydrogen fluoride (aHF). The fluorinating agents used in this study were elemental fluorine and acetyl

hypofluorite. Radiochemical techniques were applied to determine the radiochemical yield and purity of the products. Nuclear magnetic resonance (NMR) spectroscopy and mass spectrometry (MS) were used to determine the regio- and stereoselectivity of the electrophilic fluorinations.

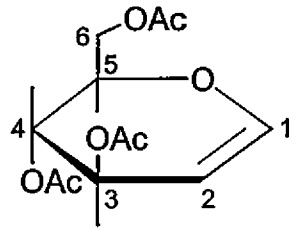

3,4,6-tri-*O*-acetyl-D-glucal (TAG)

CHAPTER 2

EXPERIMENTAL SECTION

Caution: It is recommended that proper first-aid treatment procedures[77,78,79] be known and available to all laboratory personnel prior to repeating portions of this study that deal with the use of aHF and F_2. Skin contact with even small amounts of aHF or F_2 may result in painful burns if immediate and proper treatment is not given. Any incident involving direct contact with liquid aHF, HF vapor, F_2 gas and aqueous solutions of HF must be aggressively treated and brought to the attention of qualified medical personnel for appropriate follow-up treatment.

2.1 Standard Techniques

The use of radioactive isotopes was carried out in a safe and effective manner in compliance with all requirements of the Canadian Nuclear Safety Commission (CNSC) and Radioisotope Protection Committee (RPC).

2.2 Materials

Enriched [^{18}O]O_2 (^{18}O, 99 atom%, Isotec), neon (99.999%, Air Products), 1% F_2 in neon (Canadian Liquid Air), helium (99.9999%, Matheson), anhydrous hydrogen fluoride (Air Products, 99.9%), 3,4,6-tri-*O*-acetyl-D-glucal (Aldrich, 98%), anhydrous ethyl ether (Aldrich, 99.0%) and HPLC grade acetonitrile (Caledon, 99.8%) were used without further purification and/or drying. Sterile, deionized water was used in all aqueous procedures.

2.3 Production of [^{18}F]F_2

Fluorine-18 labelled F_2 was produced by the ^{18}O(p,n)^{18}F nuclear reaction using a Siemens RDS 112 proton cyclotron operating at 11 MeV by the use of the "double shoot"

method[45] in the Nuclear Medicine Department, Hamilton Health Sciences as previously described.[55] An aluminum target (11 mL) was pressurized to 15-17 atm with 99% enriched $[^{18}O]O_2$ and irradiated for 30 min using a 30 μA proton beam (*production shoot*). After irradiation, the $[^{18}O]O_2$ was recovered from the target by condensing it at -196 °C onto molecular sieves (Varian VacSorb) contained in a 316 stainless steel Whitey® cylinder (75 mL). The target was then evacuated to remove residual ^{18}O, flushed with neon (ca. 7 atm), and re-evacuated. The target was then filled with 1% F_2 (30 – 50 μmol) in neon, pressurized to 20 atm with neon, and irradiated for 15 min in a 15 μA proton beam (*recovery shoot*). The $[^{18}F]F_2$ was sporadically released from the target into a continuous stream of helium (10 mL/min) until the target pressure dropped to 2 atm. Helium was used as the sweep gas to transfer $[^{18}F]F_2$ from the target into the hot cell and to help dissipate the heat evolved during the fluorination reaction.

2.4. Electrophilic Fluorinations of TAG in aHF Using F_2 and $[^{18}F]F_2$

For details relating to the fluorination apparatus see Figure 2.0. TAG (20 mg; 73.5 μmol) was loaded into a $^5/_{16}$" o.d. × $^5/_{32}$" i.d. FEP (perfluoroethylene/perfluoropropylene co-polymer) reaction vessel and attached to a Kel-F (trifluorochloropolyethylene polymer) Y-piece with $^1/_4$" o.d. × $^1/_8$" i.d. ends. One arm of the Y-piece was connected through a Kel-F valve to a vacuum line used to dispense aHF. A $^1/_{16}$" o.d. × $^1/_{32}$" i.d. length of Teflon tubing was fed through a $^1/_4$" o.d. × $^1/_{16}$" Teflon® Swagelok® reducing union and connected to the remaining arm of the Y-piece. The Teflon® tube was fed into and to the bottom of the FEP reaction vessel and sealed at the $^1/_{16}$" Teflon® union connection. Anhydrous HF was condensed into the

Figure 2.0. A schematic diagram of the experimental flow apparatus used for fluorination in this work.

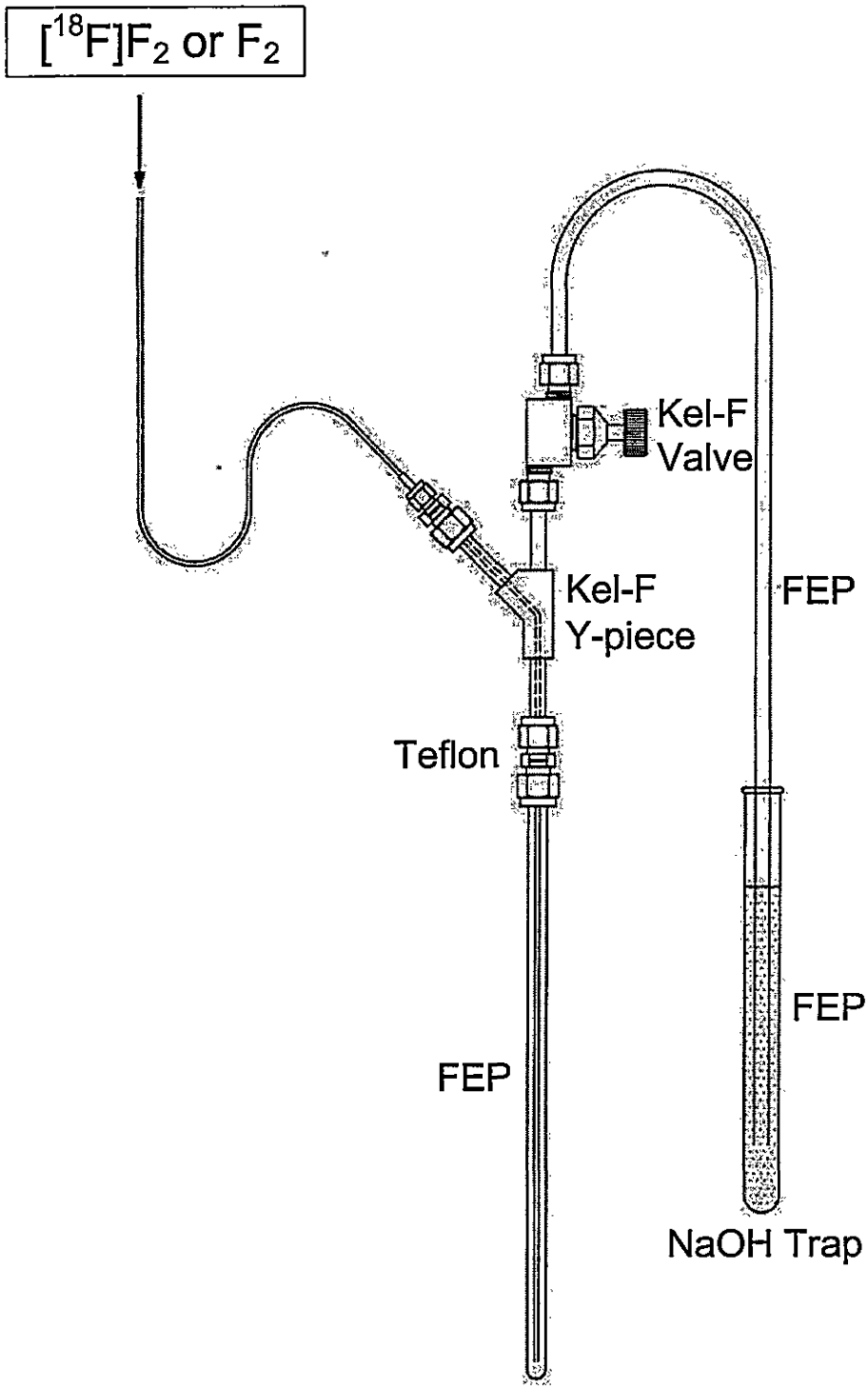
[18F]F2 or F2
Kel-F
Valve
Kel-F
Y-piece
FEP
Teflon
FEP
FEP
NaOH Trap

reaction vessel at -196 °C. The reaction vessel and contents were equilibrated at -60 °C (liquid nitrogen cooled methanol bath) and the reaction vessel was disconnected from the vacuum line. The Teflon® tube was connected to a stainless steel vacuum manifold (28.5 mL) used to dispense F_2. The initial manifold pressure of 8 atm of 1% F_2 in neon was adjusted to 27 atm with helium. The remaining arm of the Y-piece was connected to a separate $^1/_{16}$" o.d. Teflon® tube, which was led into a 1 N NaOH solution that served to trap the effluent gas as it emerged from the reaction vessel. Approximately 20 atm of the resulting F_2/Ne/He mixture was passed through the substrate solution.

When electrophilic fluorinations were carried out using $[^{18}F]F_2$, the reactor configuration remained unchanged except that the Teflon® tube was connected to the $[^{18}F]F_2$ target line. A helium sweep gas line was connected to the $[^{18}F]F_2$ target line (between the target and the reaction vessel) and a slow stream of helium was passed through the line. An aliquot of $[^{18}F]F_2$ gas was released from the target by opening the target valve and closing it intermittently. Fluorine-18 labelled F_2 gas and the helium sweep gas were passed through the reaction vessel containing the substrate solution. The effluent gas from the reaction vessel was trapped in the NaOH solution before it was vented into the hot cell. The amount of $[^{18}F]F_2$ that had reacted was determined by counting the amount of radioactivity present in the reaction mixture.

Once the desired amount of F_2 (or $[^{18}F]F_2$) gas had passed through the substrate solution, the reaction vessel was disconnected from the F_2 line (or the target) and the NaOH trap and the HF solvent was removed under dynamic vacuum and trapped in a FEP U-tube cooled to -196 °C.

2.5 Gas-Solid Phase Generation of CH_3COOF and $[^{18}F]CH_3COOF$ from $KOAc(HOAc)_{1.5}$

The complex, $KOAc(HOAc)_{1.5}$, was prepared as previously described.[67] A 2" long × $^1/_4$" o.d. × $^1/_8$" i.d. FEP column, fitted with a $^1/_4$" o.d. × $^1/_{16}$" Teflon® Swagelok® reducing union on one end and a $^1/_4$" to $^1/_{16}$" stainless steel Swagelok® reducing union on the other end, was packed to a depth of 1" with $KOAc(HOAc)_{1.5}$. The Teflon® Swagelok® union was connected to a $^1/_{16}$" o.d. stainless steel F_2 line and 8 atm of 1% F_2 in neon was diluted to 27 atm with helium inside a stainless steel vacuum manifold (28.5 mL). Approximately 20 atm of the resulting F_2/Ne/He mixture was passed through the column containing the $KOAc(HOAc)_{1.5}$ complex, which resulted in the formation of CH_3COOF gas.

In the case of $[^{18}F]CH_3COOF$, the $KOAc(HOAc)_{1.5}$ column was connected, through the Teflon® Swagelok® union, to a $^1/_{16}$" stainless steel tube leading from the $[^{18}F]F_2$ target cell. After irradiation, the target gas was slowly metered through the $KOAc(HOAc)_{1.5}$ complex, forming $[^{18}F]CH_3COOF$ gas.

2.6 Electrophilic Fluorinations of TAG in aHF using CH_3COOF and $[^{18}F]CH_3COOF$

The reaction conditions were identical to those described above. The $KOAc(HOAc)_{1.5}$ column used to generate CH_3COOF and $[^{18}F]CH_3COOF$ gas was connected to a $^1/_{16}$" o.d. × $^1/_{32}$" i.d. Teflon® tube, which was fed through one of the arms of a Kel-F Y-piece into a $^5/_{16}$" o.d. × $^5/_{32}$" i.d. FEP reaction vessel containing TAG (20 mg; 73.5 μmol) in aHF (ca. 1 mL) and connected as described above. The fluorination was carried out using the procedure described above. Once the desired amount of CH_3COOF (or $[^{18}F]CH_3COOF$) had passed through the substrate solution, the

reaction vessel was disconnected from the CH_3COOF (or $[^{18}F]CH_3COOF$) line and the NaOH trap. Anhydrous HF solvent was removed under vacuum by pumping through an FEP U-tube cooled to -196 °C.

2.7 Hydrolysis of the Reaction Intermediate Resulting from Electrophilic Fluorination of TAG

The reaction intermediate was recovered from the reaction vessel by dissolution in a 5% water/CH_3CN mixture, followed by two rinsings with the same solvent mixture. The combined rinsings were then passed through a silica Sep-Pak® (Waters Corporation, Milford, Massachusetts, USA) and collected in a 10 mL Reacti-Vial® equipped with a magnetic stirring bar. The solvent was evaporated to dryness under a slow stream of nitrogen gas in a Reacti-Therm® (Pierce) set at 130 °C. A 2.0 mL aliquot of 1 N HCl was added to the Reacti-Vial® and the residue was hydrolyzed at 130 °C for 17 min.

2.8 Separation and Purification of the Hydrolysis Product by Liquid Chromatography

A 1 cm o.d. × 17 cm long column (Bio-Rad) was packed with ion retardation resin (Bio-Rad AG® 11 A8, 50-100 mesh) and the column was washed with water. An alumina Sep-Pak® (Waters Corporation, Milford, Massachusetts, USA) was conditioned with 10 mL of water and attached to the end of the ion exchange column. A C_{18} Sep-Pak® (Waters Corporation, Milford, Massachusetts, USA) was conditioned with 4 mL of absolute ethanol followed by 10 mL of water and attached to the end of the alumina Sep-Pak®. The end of the C_{18} Sep-Pak® was attached to a 30 mL multi-dose vial through a 0.2 μm filter.

The hydrolysis product was added to the top of the LC column and eluted with 10 mL of water into a 30 mL multi-dose vial. Ionic species and unhydrolyzed organic

compounds remained on the column while the hydrolyzed product was collected in the multi-dose vial.

2.9 Radio-HPLC and Radio-TLC Analyses of 2-[^{18}F]FDβA

A 0.1 mL aliquot of the purified product solution was diluted with a 95% CH_3CN and 5% H_2O solvent mixture. In order to confirm the presence of 2-[^{18}F]FDβA and the presence of other fluorinated sugars, 0.1 mL of the diluted purified product sample was analyzed with HPLC on a carbohydrate analysis column (Waters Associates) using a 95% CH_3CN and 5% H_2O solvent mixture as the mobile phase. The flow rate was 2.0 mL/min. The eluates from the column were passed through a Beckman radioisotope detector (Model 170), which was connected to a Waters Millenium Chromatography Manager. Radiochemical contamination by ^{18}F-fluoride and unhydrolyzed ^{18}F-labelled reaction intermediates were determined by spotting the product onto a Kiesegel 60 (Merck) TLC plate and by elution with a 95% CH_3CN and 5% H_2O solvent mixture as the mobile phase. Radiochemical purity was determined by scanning the TLC strip with a chromatogram scanner (BioScan).

2.10 NMR Spectroscopy

NMR samples in 2-FDβA study were dissolved in and locked to ^{2}D in D_2O. Spectra were externally referenced with respect to neat TMS (^{1}H and ^{13}C, 25 °C) and neat $CFCl_3$ (^{19}F, 30 °C).

Proton and ^{13}C NMR spectra were recorded at 600.130 MHz and 150.903 MHz, respectively, on a Bruker Avance 600 MHz NMR spectrometer using a 5-mm triple broad band inverse probe. Sample temperatures were maintained at 25 °C by means of a BVT 3000 digital temperature controller.

Proton NMR spectra were obtained in 48 scans in 64 K data points over a 5.00 kHz spectral width corresponding to an acquisition time of 6.55 s and a digital resolution of 0.076 Hz/point. The residual HDO solvent peak was suppressed by presaturation during a 1.5 s relaxation delay between acquisitions. The data were zero-filled to 128 K before Fourier transformation. The free induction decays (FIDs) were processed using Gaussian multiplication with –2.00 Hz line broadening and Gaussian broadening of 0.1.

Proton correlation spectroscopy (COSY) spectra were recorded in the absolute value mode using the pulse sequence $90° - t_1 - 45° - \mathrm{ACQ}$ and included pulse field gradients for coherence selection. The data were acquired in 16 scans for each of the 256 FIDs that contained 2 K data points in the F_2 dimension over a 5.00 kHz spectral width. The ^{1}H 90° pulse width was 8.0 μs. A 1.0 s relaxation delay was used between acquisitions. Zero-filling in the F_1 dimension produced a 1 K x 1 K data matrix with a digital resolution of 4.88 Hz/point in both dimensions. During the 2-D Fourier transformation, a sine-bell squared window function was applied to both dimensions. The transformed data were then symmetrized.

Selective 1-D total correlation spectroscopy (TOCSY) ^{1}H spectra with pulsed field gradients were recorded over an 8.09 kHz spectral width in 64 K data points corresponding to a 4.05 s acquisition time. Selective excitation was provided by Gaussian-shaped pulses with a 180° pulse width corresponding to 83.4 ms. This pulse was followed by the standard TOCSY MLEV-17 spin-lock pulse sequence. The 90° spin-lock pulse width was 63.0 μs. A 1.0 s relaxation delay was used. The spin-lock period was 100 ms, which was followed by a *z*-filter that contained 10 variable delay

times ranging from 4 to 18 ms. The transmitter offset was adjusted to the frequency of the ^{1}H resonance being selectively excited. The spectra were acquired in 200 scans and the FIDs were processed using exponential multiplication with a 0.20 Hz line broadening and were zero-filled to 128 K of memory before Fourier transformation.

A selective 1-D COSY ^{1}H spectrum was obtained in 320 scans over an 8.09 kHz spectral width in 64 K data points corresponding to a 4.05 s acquisition time. The data were processed in the same manner as for the selective 1-D TOCSY ^{1}H spectra discussed above.

The ^{13}C NMR spectrum was acquired over a 36.231 kHz spectral width in 53100 scans in 32 K data points with an acquisition time of 0.45 s and a data point resolution of 1.11 Hz/point. The ^{13}C pulse width was 4 μs (30° pulse angle) and a relaxation delay of 0.5 s was employed. The FIDs were zero-filled to 64 K prior to Fourier transformation and were processed using exponential multiplication with a line broadening of 4.0 Hz and linear back-prediction.

An inverse-detected ^{1}H-^{13}C 2-D chemical shift correlation spectrum was acquired in the phase-sensitive mode using the pulsed field gradient version of the heteronuclear single quantum coherence (HSQC) pulse sequence. The FIDs in the F_2 (^{1}H) dimension were recorded over a 5.000 kHz spectral width in 2 K data points. The 256 FIDs in the F_1 (^{13}C) dimension were obtained over a 27.100 kHz spectral width. Each FID was acquired in 32 scans. The fixed delays during the pulse sequence were a 1.0 s relaxation delay and a delay for polarization transfer of 0.001786 s. The 90° ^{1}H and ^{13}C pulses were 8.0 and 14.0 μs, respectively. The data were processed using a sine-bell squared

window function shifted by $\pi/2$ in both dimensions and a linear prediction to 256 data points in the F_1 dimension followed by zero-filling to 1 K.

Fluorine-19 NMR spectra were recorded at 470.592 MHz on a Bruker Avance DRX-500 NMR spectrometer using a 5-mm broad band inverse probe with the ^{1}H coil tuned to the ^{19}F frequency. The spectra were obtained over a 6.887 kHz spectral width in 64 K data points corresponding to an acquisition time of 4.76 s and a data point resolution of 0.11 Hz/point. Adequate signal-to-noise was achieved in 60 scans. The ^{19}F pulse width was 2.5 μs (30° pulse angle) and a relaxation delay of 1.0 s was used. The FIDs were processed using Gaussian multiplication with -1.50 Hz line broadening and Gaussian broadening of 0.2. The data were zero-filled to 128 K before Fourier transformation. The sample temperature was maintained at 30 °C by means of a Bruker BVT 3000 digital variable temperature unit.

2.11 Mass Spectrometry

The mass spectrometric analyses were carried out on a Waters Micromass Quattro Ultima triple quadrupole mass spectrometer equipped with an electrospray ionization (ESI) interface. Samples were prepared in water, which was also used as the blank. The blank and analytes were injected by use of a pneumatically assisted Rheodyne 7010 injector equipped with a 10 μL injection loop at a flow rate of 10 μL/min.

2.12 Measurement of the Radioactivity

Radioactivity was measured using a radioisotope calibrator (Capintec CRC-12) manufactured by Capintec, Inc. It consisted of a 6 cm i.d. and 25 cm deep measuring well surrounded by an ionization chamber filled with argon gas. The chamber walls were made of aluminum and the outside wall was shielded with $^{1}/_{8}$" thick lead. The current

produced in the ionization chamber, as a result of the interaction of the ionizing radiation with the gas molecules, was recorded using a digital readout. The Capintec could measure radioactivity in the range 10 μCi up to 2 Ci with an accuracy of ±2% for γ rays with ≥0.1 MeV energies.

In the present work, the measured values for ^{18}F were decay corrected back to the end of the fluorination step of the experiment. The radioactivity present at the end of fluorination was taken to be the measured radioactivity (A_i) at zero time (t = 0). Successive measurements of the sample radioactivities (A_t) were decay corrected to the theoretical radioactivity at the end of fluorination (A_o) using eq. (2.1), where λ is defined by eq. (2.2):

$$A_o = A_t e^{\lambda t} \tag{2.1}$$

$$\lambda = (\ln 2)/t_{½} \tag{2.2}$$

where $t_{½}$ is the half-life of ^{18}F (109.7 min) and t is the time (min) from the end of fluorination up to the time when radioactivity is measured. Radiochemical yields (RCY) of the final product were reported by expressing A_o as a percentage of the measured initial activity, A_i.

2.13 Biological Studies with 2-[^{18}F]FDβA

All animal experiments were designed in accord within the guidelines of the Institutional Review Board, McMaster University and were carried out under the supervision of Dr. Troy Farncombe (Department of Radiology) and Dr. Renee Labiris (Department of Medicine) at McMaster University. Two normal Sprague-Dawley type rats and a Polynoma Middle T mouse with breast tumour were used. The rats and mouse weighed approximately 300 g and 25 g, respectively. During scanning, the animals were

anesthetized with 1-2% inhaled isoflurane. PET scanning was carried out on a Philips Mosaic small animal PET scanner.

The rats were scanned over a period of 90 min which divided into 5 min frames. A dose of 0.5-1.0 mCi of either 2-[^{18}F]FDβA or 2-[^{18}F]FDG in about 0.3 mL of saline solution was administered through the tail vein of each rat. Images were obtained by summing the entire 90 min acquisition.

The diseased mouse was scanned over a period of 60 or 90 min which was divided into 5 min frames after administration of 0.3-0.5 mCi of either 2-[^{18}F]FDβA or 2-[^{18}F]FDG in about 0.2 mL of saline solution administered through the tail vein. Images were obtained by summing the entire 60 or 90 min sequence.

CHAPTER 3

TWO-STEP REGIO- AND STEREOSELECTIVE SYNTHESIS OF 2-FLUORO-2-DEOXY-β-D-ALLOSE

3.1 Introduction

Although fluorine is incorporated into 30 known natural products,[80] fluorinated carbohydrates are extremely rare in nature. Just one fluorine-containing carbohydrate derivative, namely 4′-fluoro-5′-O-sulfamoladenoside (nucleocidin), has been isolated from an organism *Streptomyces calvus* obtained from an Indian soil sample.[81,82] However, as noted in Chapter 1, the interest in natural substance analogues containing fluorine is continually increasing owing to the modification of the chemical and biological properties as well as the selectivity of fluorine substituted molecules.[83]

Substitution of a hydroxyl group for fluorine results, in almost all cases, in molecules that are generally metabolized without C-F bond attack. Carbohydrates in which one or several hydroxyl groups are replaced by fluorine are of interest as potential antimetabolites.[84] Deoxyfluorinated sugars allow studies of carbohydrate transport and metabolism and are useful keys for the isolation of a specific biochemical reaction sequence from a general metabolic pathway, especially in the functional imaging sciences.[85] For example, whole-body PET imaging with the ^{18}F-labelled analogue of 2-deoxy-D-glucose, 2-[^{18}F]fluoro-2-deoxy-D-glucose (2-[^{18}F]FDG), enables inspection of glucose metabolism in all organ systems in a single examination and provides improved detection and staging of cancer, selection of therapy and assessment of therapeutic response.[26] As a result, 2-[^{18}F]FDG has become the most commonly used radiotracer for PET studies.

There have been several recent published reports related to the biological functions of D-allose. For example, Hossain and co-workers[86] have reported that D-allose provides very effective protection against neutrophil-related postischemic injury of liver tissue. Arnold and Silady[87] have reported that D-allose substantially inhibits segmented neutrophil production and lowers platelet count without detrimental side effects. Such characteristics make D-allose a candidate for the treatment of diseases such as chronic myelogenous leukemia. By analogy with glucose and its fluorinated derivative, 2-FDG, it appeared desirable to synthesize 2-fluoro-2-deoxy- D-allose, which, when labelled with ^{18}F, could serve as a probe of the bioactivity of D-allose.

Johansson and Lindberg[84] have reported the only synthesis of 2-fluoro-2-deoxy-D-allose prior to the present work, which was carried out by the reaction of the sugar epoxide, methyl 4,6-di-*O*-acetyl-2,3-anhydro-α-D-allopyranoside, with BF_3 in aqueous HF ("fluoroboric acid") at -70 °C. Hydrolysis and deprotection of the reaction intermediate resulted in 2-fluoro-2-deoxy-D-altrose, 68% of which was epimerized to 2-fluoro-2-deoxy-D-allose in 33% aqueous trimethylamine at 60 °C over a period of 5 h. The final reaction product was a mixture of the α- and β-anomers. This lengthy and multi-step synthesis of 2-fluoro-2-deoxy-D-allose cannot be used to synthesize the ^{18}F-lablled analogue of the compound. Although the authors referred to unpublished ^{1}H and ^{19}F NMR data to support their structural characterization, no NMR parameters were provided.

Carbohydrates in which a primary hydroxyl group is replaced by fluorine have been prepared from the sulfonates, but this reaction cannot be used for the introduction of fluorine at secondary positions.[84] The synthesis of carbohydrates bearing fluorine at

secondary positions, especially at C2, however, has been of interest for many years owing to their importance in biochemical studies and medicinal chemistry research.[88] One of the most prevalent synthetic procedures to introduce fluorine at C2 in carbohydrate molecules is electrophilic addition of fluorine to glycals. Such reactions often show high regio- and stereoselectivity in addition reactions.[83]

Introduction of a fluorine atom at C2 by addition to glycals is effected by so-called "electrophilic fluorinating reagents, $R^{\delta-}$–$F^{\delta+}$". Because C2 of a glycal is more electronegative than C1 as a result of resonance contributions –O–C(1)=C(2) ↔ $-O^{+}$=C(1)–C^{-}(2), the fluorine of R–F always adds to C2. Reagents in this category include CF_3OF, F_2 diluted with an inert gas, CH_3COOF and XeF_2.[89] Because almost all electrophilic fluorinating agents are the products of direct fluorination by F_2, it is desirable to use F_2 directly as the electrophilic fluorinating agent, thereby eliminating additional synthetic step(s).

Adamson and co-workers[90,91] first reported the syntheses of 2-fluoro-2-deoxy sugars by addition of CF_3OF to 3,4,6-tri-*O*-acetyl-D-glucal (TAG) dissolved in $CFCl_3$ at -80 °C followed by acid catalyzed hydrolysis of the reaction intermediates. The syntheses produced 2-fluoro-2-deoxy-D-glucose (2-FDG) and 2-fluoro-D-mannose (2-FDM) in good yields. Since then, TAG has been one of the most widely used precursors for the syntheses of 2-fluoro-2-deoxy sugars.

Lundt and Pedersen[92-94] extensively studied the reactions of TAG and other 3,4,6-tri-*O*-substituted glycals with and in anhydrous hydrogen fluoride (aHF) solvent and in mixed solvent media containing HF. The reaction of TAG with aHF resulted in a 1,2-unsaturated 3,4-dioxolenium ion, which was stable in aHF at -70 °C for several

hours. After a period of 24 h, it was found that HF had added across the double bond of the dioxolenium ion. Extraction of HF, followed by addition of water hydrolyzed the intermediate and epimerization occurred at C3, with the configuration at C3 changing from *S* in the starting material to *R* in the product.[92]

Drawing on the synthetic approach of Lundt and Pedersen[93] and the established synthetic procedure used to introduce fluorine at C2 in hexapyranoses, [90,91,95-97] a rapid and efficient two-step synthesis of 2-(*R*)-fluoro-2-deoxy-β-D-allose (2-FDβA), resulting from electrophilic fluorination of TAG, is reported in this Chapter. A detailed ^{1}H, ^{13}C, and ^{19}F NMR study has provided the first unambiguous structural characterization of 2-FDβA.

3.2 Results and Discussion

3.2.1 Choice of Fluorinating Agents

Elemental fluorine and AcOF were chosen as the electrophilic fluorinators in this study mainly because these agents are most commonly used for the electrophilic syntheses of 2-deoxy-2-fluoro-sugars starting from TAG. In addition, there have been several comparative studies of the reactivity and selectivity of these fluorinating agents towards TAG.[98] Acetyl hypofluorite shows some important differences in reactivity, relative to F_2, in that it is a milder and more selective reagent. Thus, it was expected that AcOF would produce fewer fluorinated and/or non-fluorinated by-products when reactions are carried out in acidic media in this study.

3.2.2 Synthesis of 2-FDβA

The synthesis of 2-FDβA was accomplished by electrophilic fluorination of commercially available TAG with F_2 and CH_3COOF in aHF at -60 °C, followed by acid

catalyzed hydrolysis and purification using liquid chromatography (Scheme 3.1). The compound was characterized by conventional 1-D ^{1}H, ^{13}C, and ^{19}F NMR spectroscopy and selective 1-D ^{1}H and 2-D correlation spectroscopy experiments and by mass spectrometry.

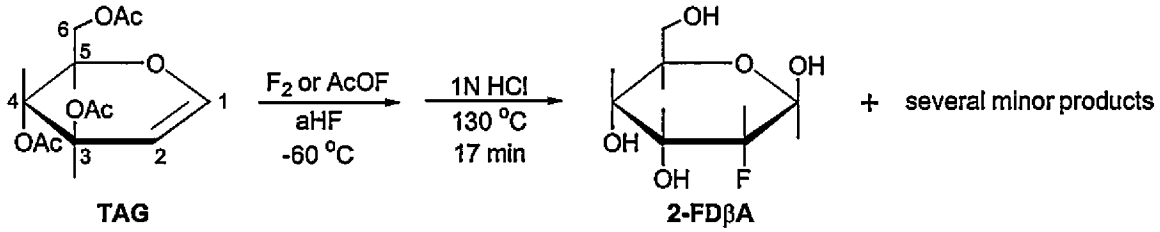

Scheme 3.1. Synthesis of 2-*(R)*-fluoro-2-deoxy-β-D-allose (2-FDβA).

3.2.3 Structural Characterization of 2-FDβA by 1-D and 2-D NMR Spectroscopy

The structures of monosaccharides and fluorinated monosaccharides can be readily analyzed, in most instances, by conventional 1-D NMR techniques and by reference to the ^{1}H and ^{13}C NMR parameters of related compounds.[99] The 1-D ^{1}H NMR spectrum (Figure 3.1) of the products of Scheme 3.1 was too complex to permit full and unambiguous analysis and extraction of NMR parameters. Only the ^{1}H resonances corresponding to the anomeric proton could be readily assigned. The full NMR structural characterization of 2-FDβA was accomplished by carrying out selective 1-D ^{1}H and 2-D correlation spectroscopy experiments.

^{1}H and Selective 1-D ^{1}H NMR and 2-D Correlation Spectroscopy

The ^{1}H NMR parameters for 2-FDβA are summarized in Table 3.1. It was evident from the ^{1}H NMR spectrum that 2-FDβA was the major carbohydrate product synthesized in Scheme 3.1. The doublet of doublets (dd) centered at 5.21 ppm was assigned to the anomeric proton, H1. The smaller coupling (1.4 Hz) is characteristic of an axial-equatorial coupling between H1 and F, and established that the fluorine atom

Figure 3.1. The ^{1}H NMR spectrum (D_2O solvent at 25 °C) of the products resulting from the electrophilic fluorination of TAG in aHF. The spectrum was processed using Gaussian multiplication and presaturation of the HDO solvent resonance at 4.77 ppm. Dots (•) and asterisks (*) and denote H4 and H6′ resonances, respectively. The dagger (†) denotes an unassigned "triplet" ($\delta(^{1}H)$ 4.39 ppm; 1.6 Hz splitting).

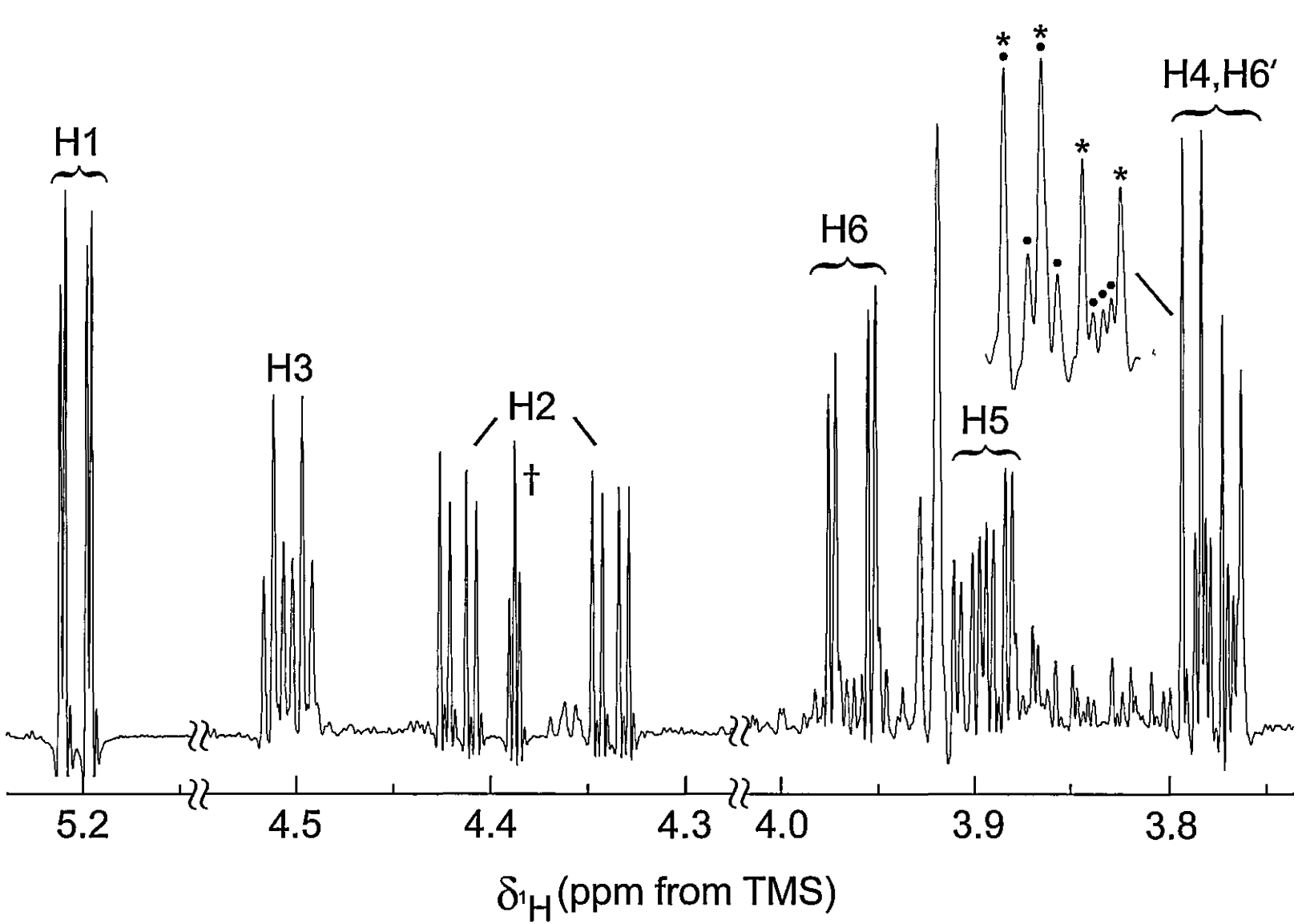
H1
H3
H2
†
H6
H5
H4,H6′
*
5.2
4.5
4.4
4.3
4.0
3.9
3.8
δ¹H (ppm from TMS)

was bonded to C2. Moreover, the larger coupling (8.2 Hz) showed that the monosaccharide possessed a *trans*-diaxial arrangement of hydrogen atoms at C1 and C2. As a result, the absolute configuration at C1 was assigned as *R*, i.e., the compound had the β-D-conformation.

Table 3.1. ^{1}H NMR Parameters for 2-FDβA.

^{1}H chemical shift (ppm)		multiplicity[a]	coupling constant (Hz)	
H1	5.21	dd	$^{3}J_{H1,F}$, 1.4	$^{3}J_{H1,H2}$, 8.2
H2	4.38	ddd	$^{2}J_{H2,F}$, 47.0	$^{3}J_{H2,H3}$, 3.1
H3	4.51	ddd[b]	$^{3}J_{H3,F}$, 8.9	$^{3}J_{H3,H4}$, 3.0
H4	3.78	ddd	$^{4}J_{H4,F}$, 1.6	$^{3}J_{H4,H5}$, 10.0
H5	3.90	ddd	$^{3}J_{H5,H6}$, 2.3	$^{3}J_{H5,H6'}$, 5.8
H6	3.97	dd	$^{2}J_{H6,H6'}$, 12.3	
H6′	3.78	dd		

[a]The abbreviations denote doublet of doublets (dd) and doublet of doublets of doublets (ddd).
[b]This multiplet appears as a doublet of "triplets" because $^{3}J_{H3,H4} \approx {}^{3}J_{H2,H3}$.

A ^{1}H-^{1}H gradient COSY spectrum (Figure 3.2) showed strong correlations between the H1 resonance and the two sets of doublet of doublets at 4.34 and 4.42 ppm. Because H1 would be coupled to only H2, two separate selective 1-D TOCSY experiments were carried out to determine which of the two doublet of doublets patterns corresponded to H2. First, the signal at 4.34 ppm was used as the starting point for the magnetization transfer. The resulting selective 1-D TOCSY spectrum (Figure 3.3) indicated that the proton corresponding to the signal at 4.34 ppm was strongly correlated

Figure 3.2. The ^{1}H-^{1}H gradient COSY spectrum (D_2O solvent at 25 °C) of the products resulting from the electrophilic fluorination of TAG in aHF.

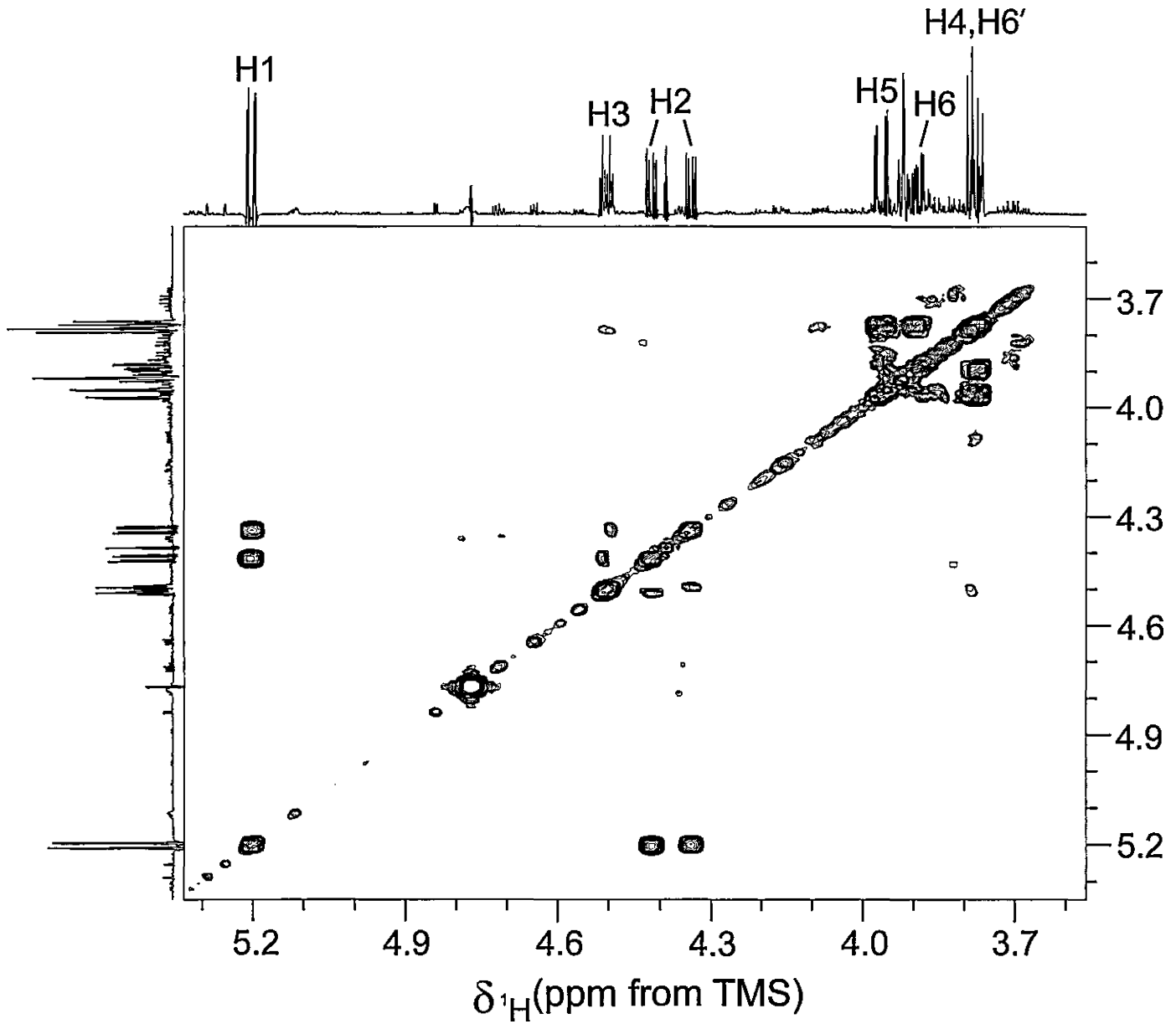
H1
H3
H2
H5
H6
H4,H6′
3.7
4.0
4.3
4.6
4.9
5.2
5.2
4.9
4.6
4.3
4.0
3.7
δ ¹H(ppm from TMS)

Figure 3.3. A selective 1-D TOCSY (D_2O solvent at 25 °C) spectrum resulting from selective irradiation at 4.34 ppm.

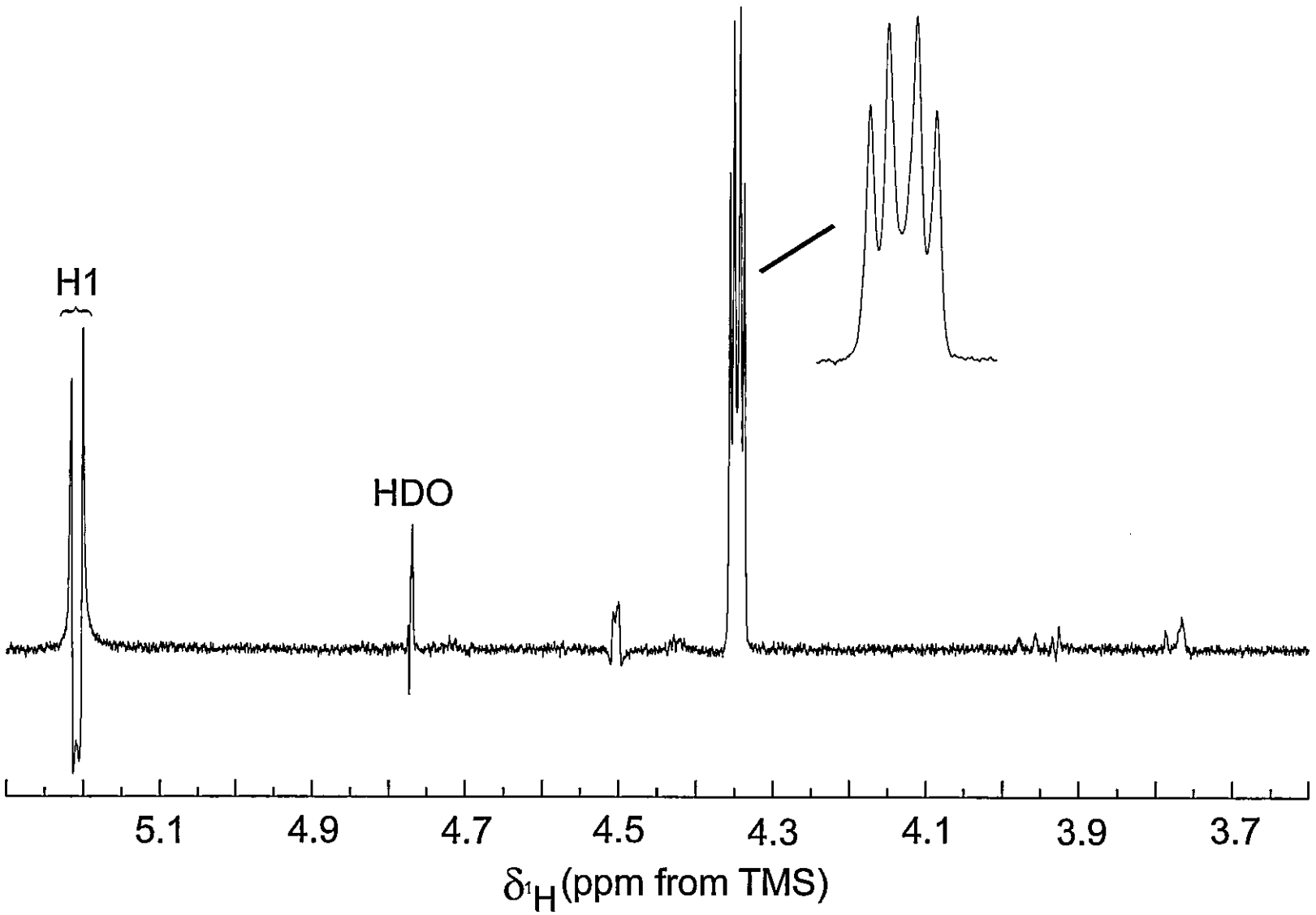
H1
HDO
5.1
4.9
4.7
4.5
4.3
4.1
3.9
3.7
δ1H (ppm from TMS)

Figure 3.4. A selective 1-D TOCSY (D_2O solvent at 25 °C) spectrum resulting from selective irradiation at 4.42 ppm.

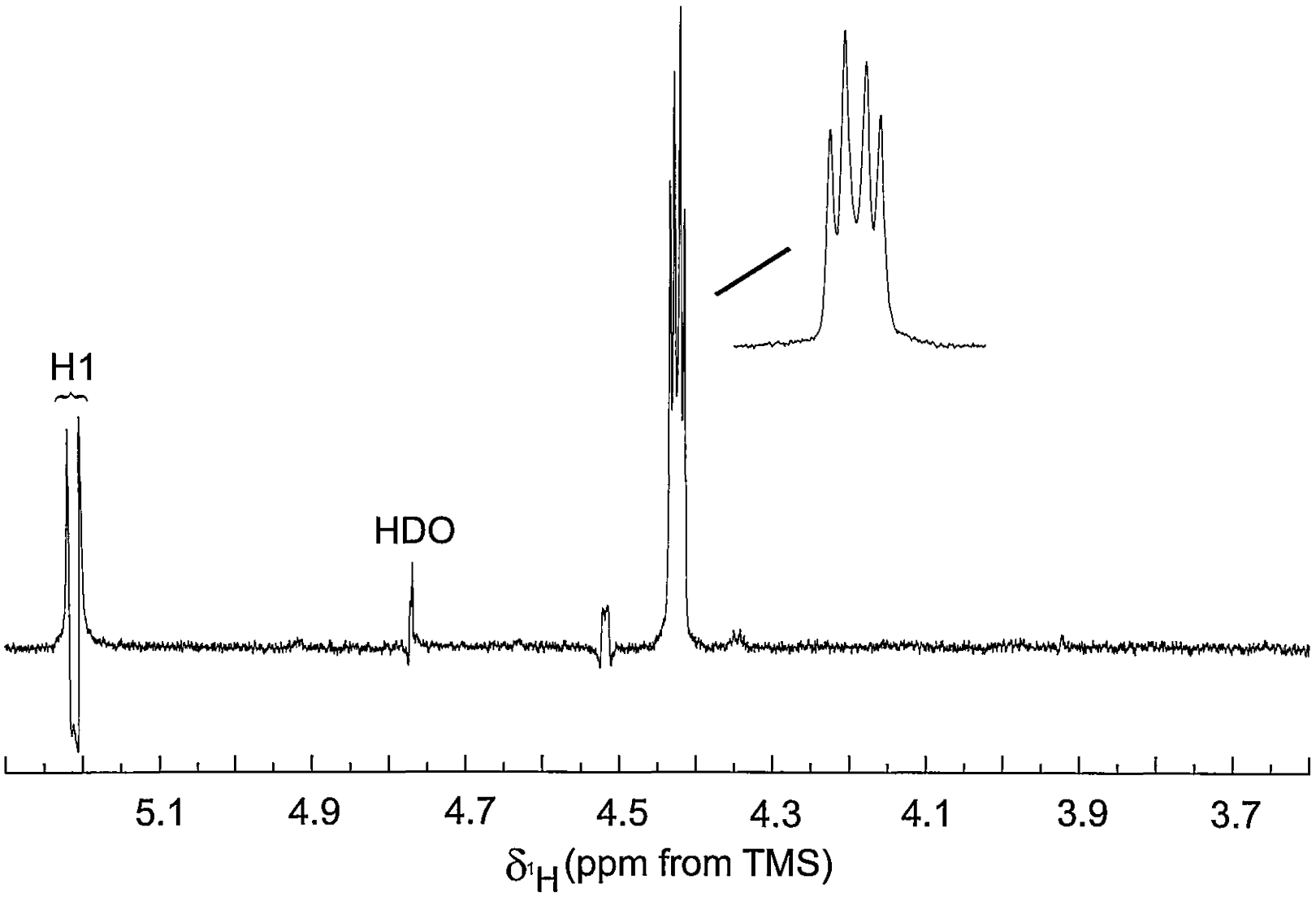
H1
HDO
5.1
4.9
4.7
4.5
4.3
4.1
3.9
3.7
δH (ppm from TMS)

with H1 and more weakly correlated with the proton corresponding to the signal at 4.51 ppm. Next, the signal at 4.42 ppm was chosen for selective irradiation. The resulting selective 1-D TOCSY spectrum (Figure 3.4) gave results identical to the previous experiment (Figure 3.3). No correlation was, however, observed between the signals used for the selective 1-D TOCSY experiments. From these findings, as well as the measured coupling constants, both of the signals at 4.34 and 4.42 ppm were assigned to H2 and the overall multiplicity was a doublet of doublets of doublets centered at 4.38 ppm. The 47.0 Hz coupling confirmed that fluorine was bonded to C2. The magnitudes of the $^{2}J_{H2,F}$, $^{3}J_{H2,H1}$ and $^{3}J_{H2,H3}$ couplings unequivocally established the absolute configuration at C2 as *R*.

The ^{1}H-^{1}H COSY and selective 1-D TOCSY experiments were also used to assign the H3 resonance to the doublet of pseudo-triplets at 4.51 ppm. The larger (8.9 Hz) coupling is characteristic of equatorial-equatorial coupling between H3 and fluorine bonded to C2. Each pseudo-triplet arose from the overlap of two sets of doublets having an average *J*-value of 3.0 Hz and resulted from the three-bond equatorial-axial couplings, $^{3}J_{H2,H3}$ and $^{3}J_{H3,H4}$. The magnitudes of $^{3}J_{H3,F}$, $^{3}J_{H3,H2}$ and $^{3}J_{H3,H4}$ confirmed the *R*-configuration at C3.

In addition to correlation between H2 and H3, the ^{1}H-^{1}H COSY spectrum showed correlation between H3 and the proton(s) responsible for the complex multiplet centered at 3.78 ppm. Although it was certain that this multiplet included the H4 resonance, it was apparent from peak integration that the multiplet corresponded to two hydrogen atoms. A selective 1-D COSY experiment (Figure 3.5) proved that the multiplet's complexity and

Figure 3.5. The selective 1-D COSY (D_2O solvent at 25 °C) spectrum resulting from selective irradiation at 4.51 ppm.

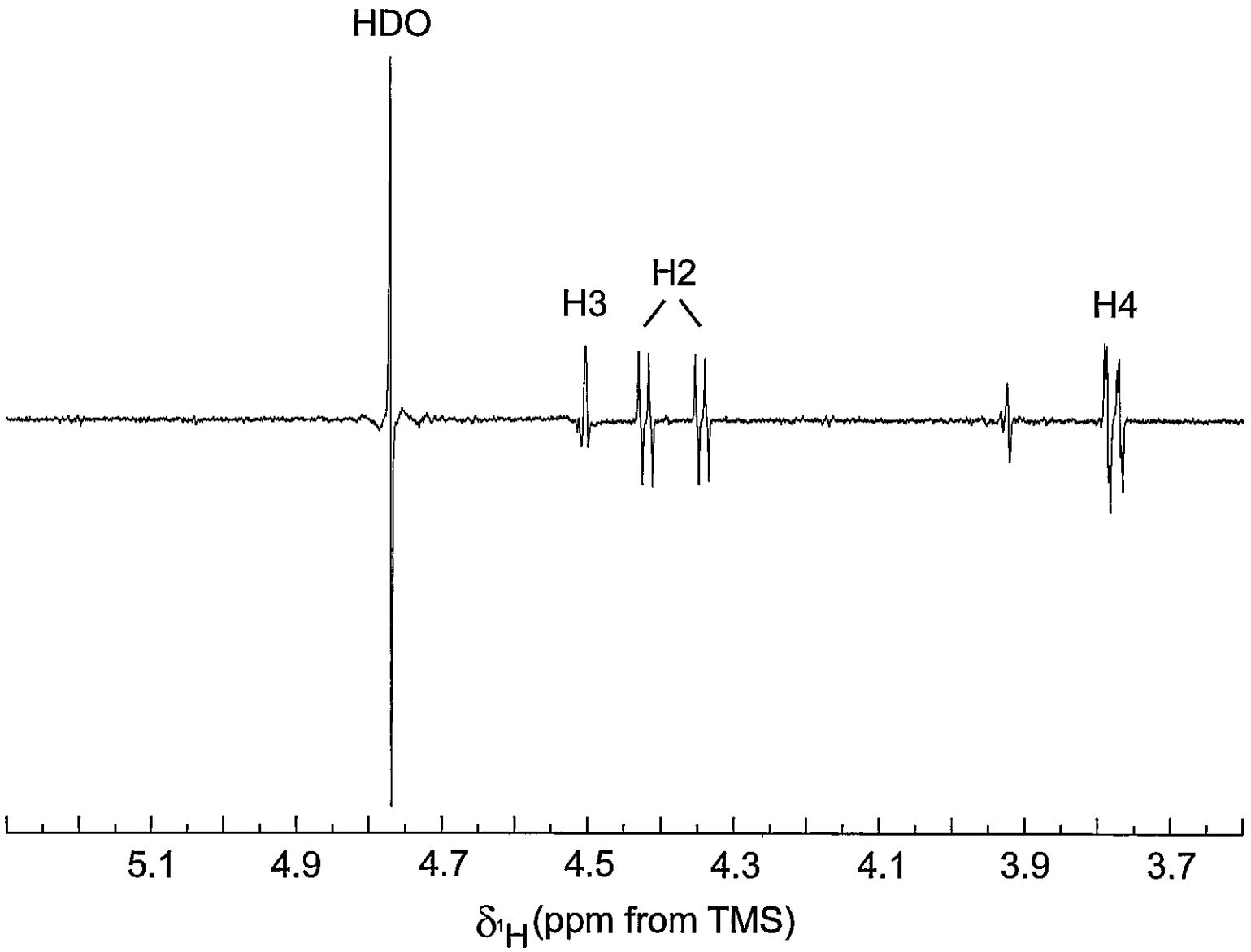
HDO
H3
H2
H4
5.1
4.9
4.7
4.5
4.3
4.1
3.9
3.7
δ1H (ppm from TMS)

integrated intensity resulted from overlap of the resonances corresponding to H4 and another proton. The magnitudes of the *trans*-diaxial coupling between H4 and H5 (10.0 Hz) and the three-bond axial-equatorial coupling between H4 and H3 (3.0 Hz) confirmed that the absolute configuration at C4 was *R*. A long-range coupling (1.4 Hz) between H4 and the fluorine bonded to C2 was also observed.

The H5 and the diastereotopic H6 and H6′ resonances were assigned by the use of the magnitude of the coupling between H4 and H5 as well as by the ^{1}H-^{1}H COSY experiment. The doublet of doublets centered at 3.90 ppm was assigned to H5. As noted above, the 10.0 Hz coupling arose from $^{3}J_{H5,H4}$. The two smaller couplings, 5.8 and 2.3 Hz resulted arose from the three-bond coupling to the diastereotopic H6 (3.97 ppm) and H6′ (3.78 ppm) protons.

1-D ^{13}C NMR and 2-D Correlation Spectroscopy

Assignments of the ^{13}C resonances (Figure 3.6 and Table 3.2) were aided by the ^{13}C-^{19}F coupling constants and by a ^{13}C-^{1}H heteronuclear single quantum correlation (HSQC) experiment (Figure 3.7). The ^{13}C NMR spectrum provided further evidence that Scheme 3.1 produced 2-FDβA as the major carbohydrate product. The ^{13}C resonance of the anomeric carbon, C1, appeared as a doublet (d) at the highest frequency, 91.93 ppm, with $^{2}J_{C1,F}$ = 24.5 Hz. The chemical shift of C2, bearing the fluorine ligand and being adjacent to the anomeric carbon atom, occurred at 90.67 ppm and gave rise to a one-bond ^{13}C-^{19}F coupling (185.5 Hz) that was consistent with fluorine bonded to an sp^{3} hybridized carbon. The carbon-3 resonance appeared at 70.09 ppm and the magnitude of the $^{2}J_{C3,F}$ coupling was 15.9 Hz. The three-bond coupling between C4, which appeared at

Figure 3.6. The ^{13}C NMR spectrum (D_2O solvent at 25 °C) of the products resulting from the electrophilic fluorination of TAG in aHF.

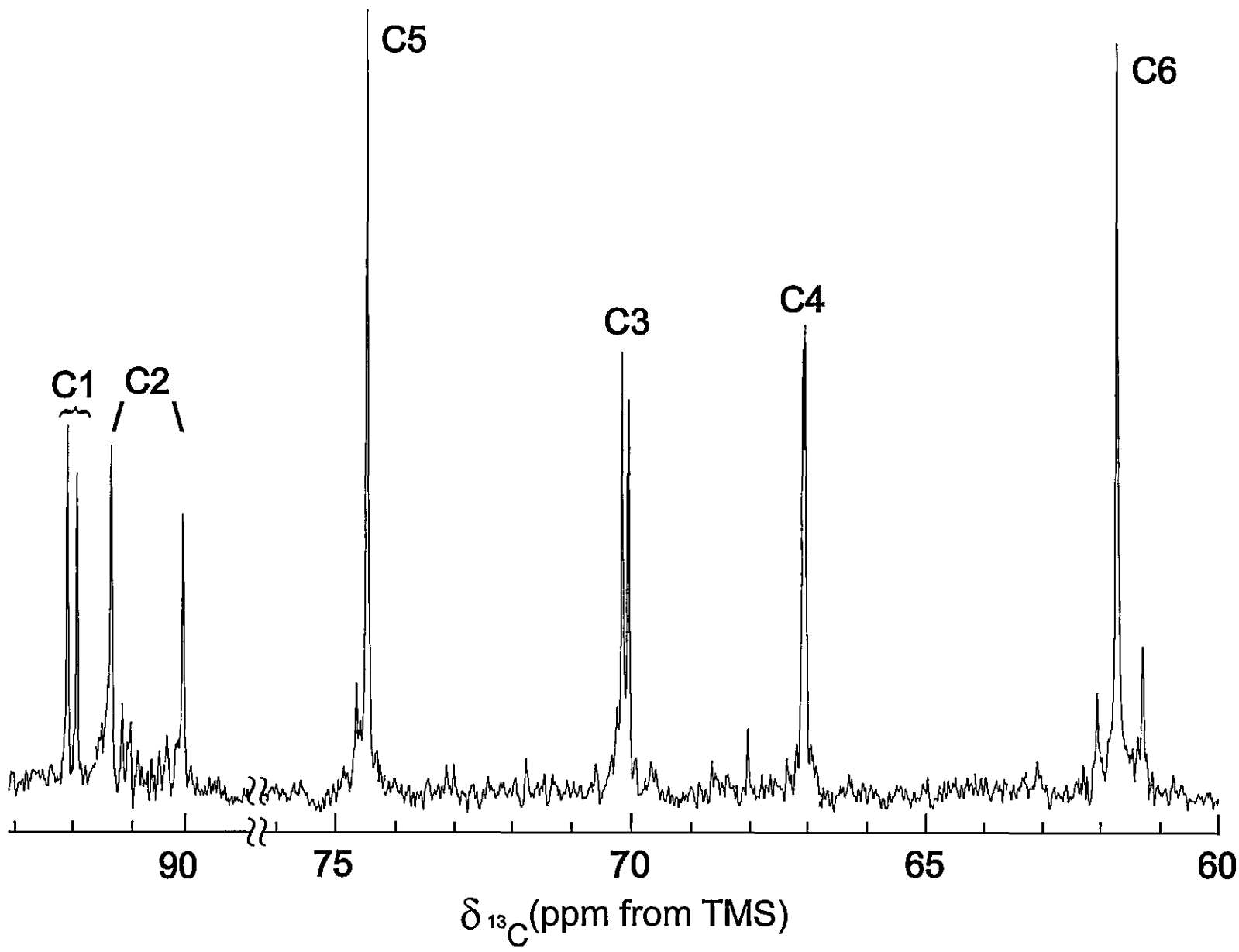
C5
C6
C4
C3
C1
C2
90
75
70
65
60
δ 13C(ppm from TMS)

Figure 3.7. The ^{13}C-^{1}H HSQC spectrum (D_2O solvent at 25 °C) of the products resulting from the electrophilic fluorination of TAG in aHF.

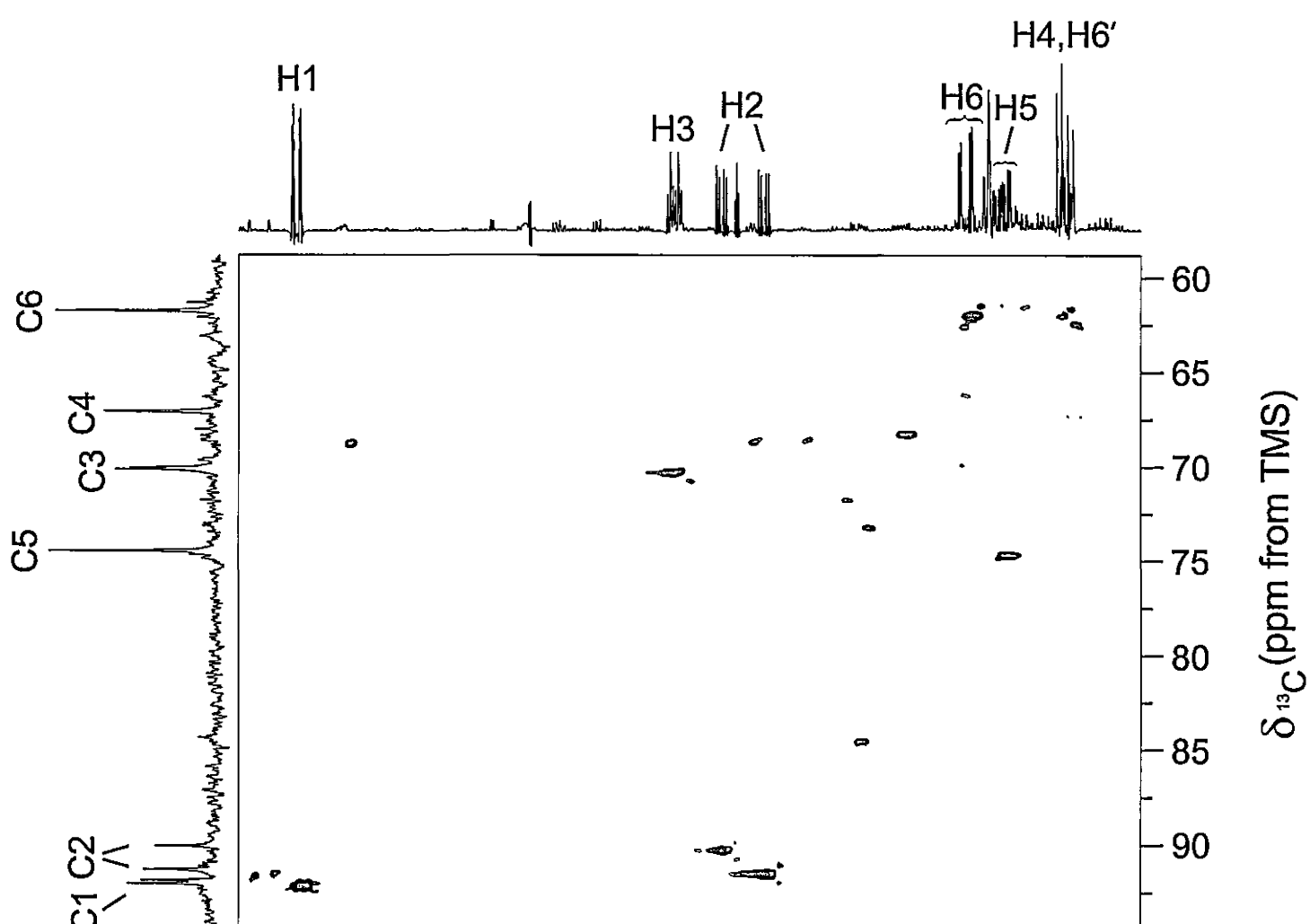
H1
H3
H2
H6
H5
H4,H6′
C6
C3 C4
C5
C1 C2
60
65
70
75
80
85
90
δ13C (ppm from TMS)
5.2
4.9
4.6
4.3
4.0
3.7
δ1H (ppm from TMS)

67.05 ppm, and the fluorine environment was 5.5 Hz. The chemical shift of C5 (74.47 ppm) appeared at higher frequency than C3 and C4 resonances, because C5 is bonded to the ring oxygen. The C6 resonance (61.75 ppm) appeared at the lowest frequency.

Table 3.2. ^{13}C NMR Parameters for 2-FDβA.

	^{13}C chemical shift[a] (ppm)		multiplicity[b]	coupling constant (Hz)
C1	91.93	(96.4)	d	$^{2}J_{C1,F}$, 24.5
C2	90.67	(74.2)	d	$^{1}J_{C2,F}$, 185.5
C3	70.09	(74.3)	d	$^{2}J_{C3,F}$, 15.9
C4	67.05	(69.5)	d	$^{3}J_{C4,F}$, 5.5
C5	74.47	(76.5)	s	
C6	61.75	(64.1)	s	

[a]Chemical shifts in parentheses are those of β-D-allose.[100]
[b]The abbreviations denote doublet (d) and singlet (s).

1-D ^{19}F NMR Spectroscopy

The 1-D ^{19}F NMR spectrum of the products (Figure 3.8) showed an intense doublet of doublets of pseudo-triplets centered at -199.99 ppm, corresponding to 2-FDβA, along with a weak, unassigned doublet of doublets centered at -199.44 ppm. The largest coupling (47.0 Hz) was assigned to the two-bond coupling between fluorine and H2. The three-bond coupling between fluorine and H3 was 8.2 Hz. Finally, the pseudo-triplet resulted from overlap of two doublets (average *J*-value, ca. 1.4 Hz) corresponding to $^{3}J_{F,H1}$ and $^{4}J_{F,H4}$. The 1-D ^{19}F NMR spectrum confirmed that 2-FDβA

Figure 3.8. The ^{19}F NMR spectrum (D_2O solvent at 30 °C) of the products resulting from the electrophilic fluorination of TAG in aHF. The spectrum was processed using Gaussian multiplication. Asterisks (*) denotes an unassigned resonance ("doublet of doublets") arising from a minor component ($\delta(^{19}F)$, -199.44 ppm; $^{2}J_{F,H}$, 44.35 Hz and $^{3}J_{F,H}$, 7.67 Hz) characteristic of a fluorocarbohydrate.

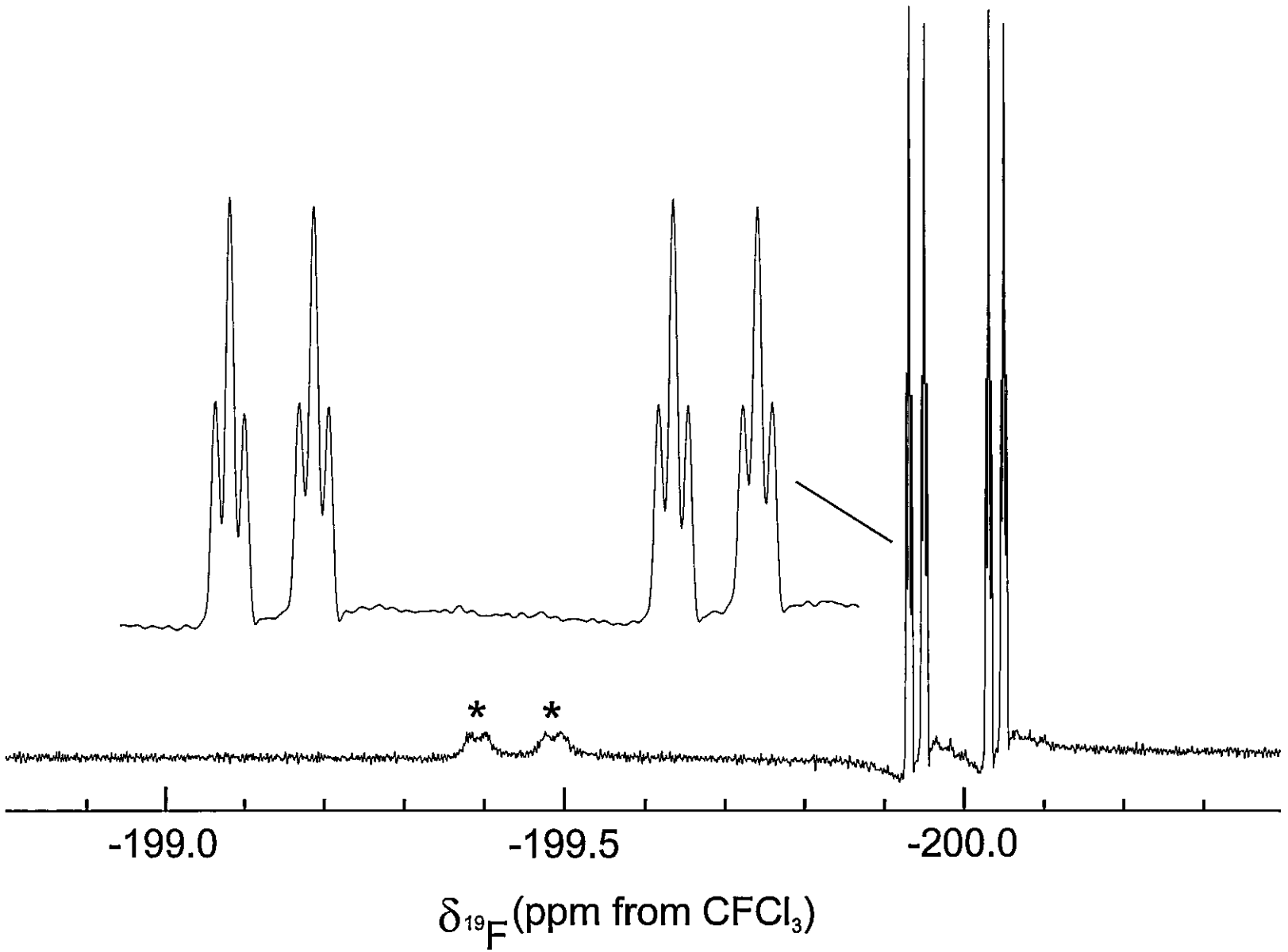
*
*
-199.0
-199.5
-200.0
δ19F (ppm from CFCl3)

was the major product of the electrophilic fluorination of TAG in aHF. It is significant that neither 2-FDG nor 2-FDM was produced in this reaction, whereas electrophilic fluorinations of TAG with F_2 and AcOF in any other solvent medium result in both 2-FDG and 2-FDM[62,65,96,101-103] (also see Chapter 4).

3.2.4 Mass Spectrometric Results

Negative ion electrospray ionization (ESI) mass spectrometry of the reaction products resulting from Scheme 1 also confirmed that 2-FDβA was the major product. The spectrum (Figure 3.9) showed the deprotonated molecular ion, $[M-H]^-$, corresponding to 2-FDβA at *m/z* 181. However, the base peak in the spectrum appeared at *m/z* 217, which corresponds to the chloride adduct of neutral 2-FDβA.

3.3 Conclusion

A reliable and rapid two-step highly regio- and stereoselective synthesis of 2-FDβA by electrophilic fluorination of TAG in aHF has been achieved. The high regioselectivity results from exclusive fluorination at C2. Stereoselectivity resulted in an *R* configuration at C2 of the product, whereas all other known electrophilic fluorinations of TAG result in products having both *R* and *S* configurations at C2. Such high regio- and stereoselectivities are often hard to achieve from electrophilic fluorinations. The total synthesis time was approximately 45 min, which is more rapid and efficient than the existing synthesis of 2-fluoro-2-deoxy-D-allose reported by Johansson and Lindberg.[84]

Figure 3.9. The ESI mass spectrum of the products resulting from the electrophilic fluorination of TAG in aHF.

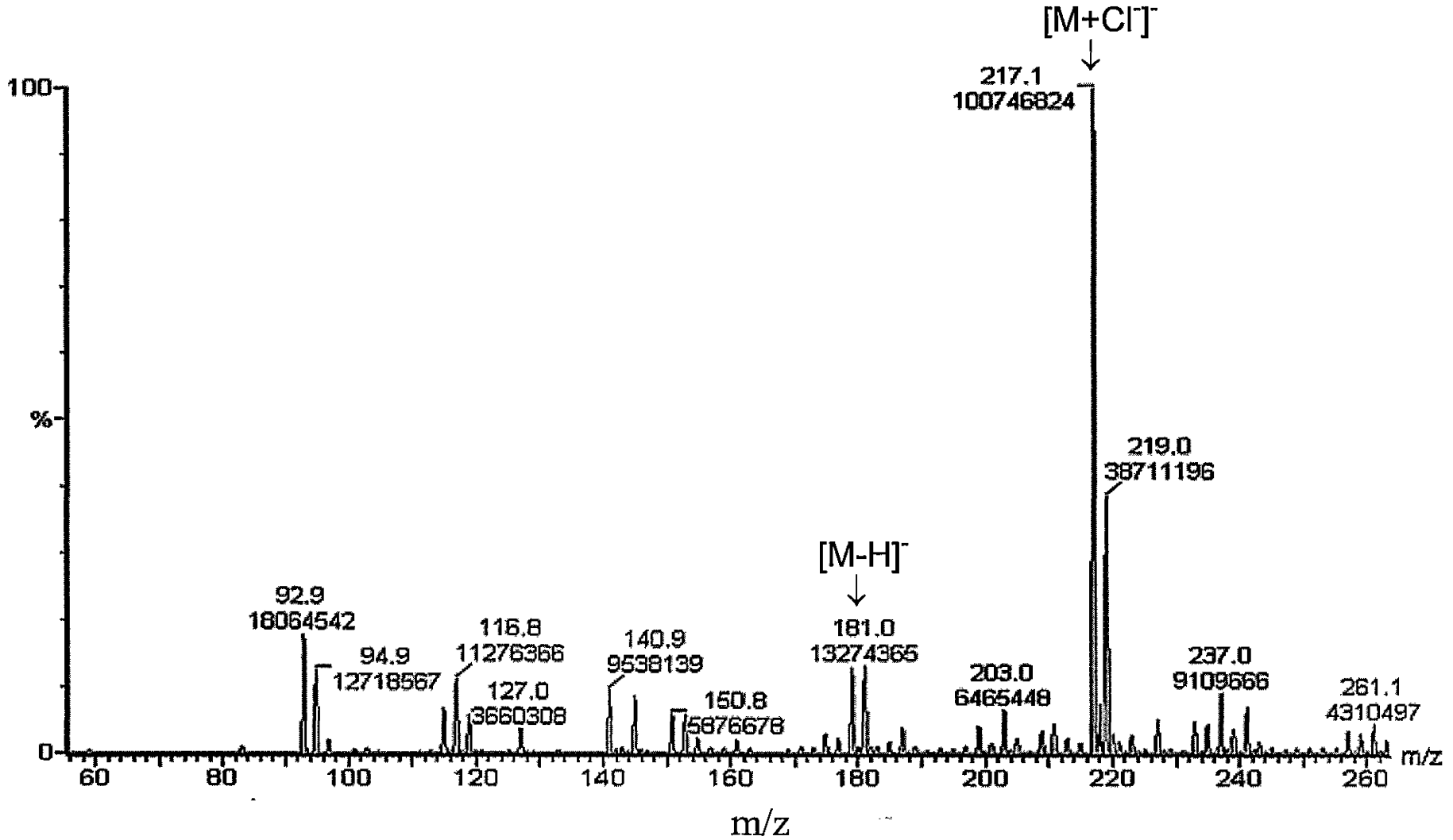
[M+Cl]⁻
217.1
100746824
219.0
38711196
[M-H]⁻
181.0
13274365
92.9
18064542
94.9
12718567
116.8
11276366
127.0
3660308
140.9
9538139
150.8
5876678
203.0
6465448
237.0
9109666
261.1
4310497
100
%
0
60
80
100
120
140
160
180
200
220
240
260
m/z
m/z

CHAPTER 4

THE SYNTHESIS OF ^{18}F-LABELLED 2-FLUORO-2-DEOXY-β-D-ALLOSE

4.1 Introduction

Radiofluorinated carbohydrates have been of significant interest in the field of nuclear medicine owing to the synthesis of 2-[^{18}F]fluoro-2-deoxy-D-glucose (2-[^{18}F]FDG) and its application in PET for the measurement of glucose metabolic rates in humans. The method allows all organ systems to be examined in a single study. Since its introduction by Ido and co-workers[95] in 1977, 2-[^{18}F]FDG has grown to be the single most important radiopharmaceutical used in PET imaging and has become the standard, with which many PET radiopharmaceuticals are compared.

The continuous success of 2-[^{18}F]FDG as a clinical and research radiopharmaceutical has prompted chemists over the years to attempt to develop syntheses for other ^{18}F-labelled carbohydrates that might find application as PET radiotracers. For example, 2-[^{18}F]fluoro-2-deoxy-galactose has been synthesized for imaging galactose metabolism in tumours such as those of the liver.[104,105]

The development of a rapid two-step regio- and stereoselective synthesis and full characterization of 2-fluoro-2-deoxy-D-allose (2-FDβA) has been described in Chapter 3. The purpose of the present study was three fold: (1) to develop the first synthesis of ^{18}F-labelled 2-FDβA (2-[^{18}F]FDβA) by use of the synthetic procedure described in Chapter 3, (2) to make use of the radiochemical synthesis to establish the reaction mechanism leading to 2-FDβA, and (3) to determine the potential use of 2-[^{18}F]FDβA as a PET radiotracer.

4.2 Results and Discussion

4.2.1 Synthesis of 2-[^{18}F]FDβA

Fluorine-18 labelled 2-FDβA (2-[^{18}F]FDβA) was synthesized by electrophilic fluorination of TAG with [^{18}F]F_2 and [^{18}F]AcOF in aHF at -60 °C, followed by acid catalyzed hydrolysis and purification using liquid chromatography (Scheme 4.1). Once the radioactivity had decayed, the compound was characterized in a manner identical to that described in Chapter 3.

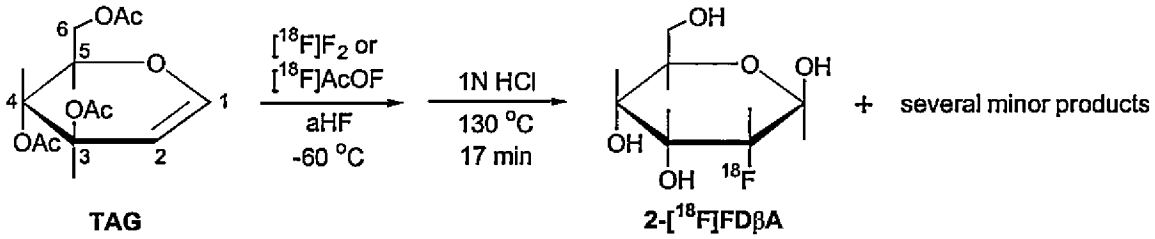

Scheme 4.1 Synthesis of 2-[^{18}F]FDβA by electrophilic radiofluorination of TAG in aHF.

The decay-corrected overall radiochemical yields (RCY) of the final product solutions were 33 ±3% and 9 ±2% with respect to [^{18}F]F_2 when [^{18}F]F_2 and [^{18}F]AcOF, respectively, were used as the fluorinating agents. The decay-corrected RCY of 33 ±3% with respect [^{18}F]F_2 is the highest RCY achieved to date for electrophilic fluorination of TAG using [^{18}F]F_2 in any solvent system. Furthermore, ^{19}F NMR studies confirmed that neither 2-FDG nor 2-FDM were produced. The former, as stated earlier, is widely used for the study of local glucose metabolism in humans and the latter is a significant contaminant when 2-[^{18}F]FDG is produced by electrophilic fluorination methods. The absence of 2-[^{18}F]FDG and 2-[^{18}F]FDM in 2-[^{18}F]FDβA is a significant factor when used for PET imaging purposes because the presence of either contaminant would contribute to background noise, reducing the signal-to-noise ratio in the resulting image, and would unnecessarily increase the radiation dose to the patient.

4.2.2 Determination of Radiochemical Purity of 2-[^{18}F]FDβA by Radio-HPLC and Radio-TLC

The radiochemical purity of 2-[^{18}F]FDβA was 96.3 ±3% and 91 ±8%, as determined by the use of radio-HPLC and radio-TLC, respectively. As expected from their structural similarities, 2-[^{18}F]FDβA had chromatographic properties similar to those of 2-[^{18}F]FDG. Figures 4.1 and 4.2 show the radioactive HPLC trace and radio-TLC chromatograms, respectively, of 2-[^{18}F]FDβA and 2-[^{18}F]FDG. The retention time (t_R) of 2-[^{18}F]FDβA was 3.83 min (Figure 4.1 a)), whereas that of 2-[^{18}F]FDG was 3.75 min (Figure 4.1 b)). The dark spots on the TLC plates (Figure 4.2) correspond to the ^{18}F radioactivity, which gave rise to the peaks on the corresponding TLC chromatograms. The R_f values for 2-[^{18}F]FDβA and 2-[^{18}F]FDG were 0.37 and 0.36, respectively.

4.2.3 Proposed Mechanistic Route to 2-FDβA Based on ^{18}F Radioactivity

Fluorination of glycals by F_2 and AcOF in polar solvents and aqueous solutions usually results in difluoro and 2-fluoro-2-deoxy intermediates, respectively, in which the electrophilic fluorinating agent is added across the double bond to give a *syn*-arrangement.[95-97] The absence of an *anti*-isomer is attributed to the fact that, unlike other halogens, fluorine cannot form a halonium ion. Therefore, the initial fluorocarbonium ion intermediate resulting from electrophilic attack of C2 by fluorine is not bridged[106] and the carbonium ion rapidly combines with the counter ion, F^- or AcO^-. Both the fluorine ligand and acetoxy group on C1 are susceptible to hydrolysis in dilute acid media.

Lundt and Pedersen[93] proposed that the reaction of TAG with aHF (Scheme 4.2) proceeded by protonation of the oxygen atom bonded to C3 and subsequent cleavage of the *O*-acetyl group was likely assisted by attack from the acyloxy group at C4. These

Figure 4.1. Radio-TLC chromatograms and plates of (a) the products resulting from the electrophilic fluorination of TAG in aHF and (b) 2-[^{18}F]FDG.

a)

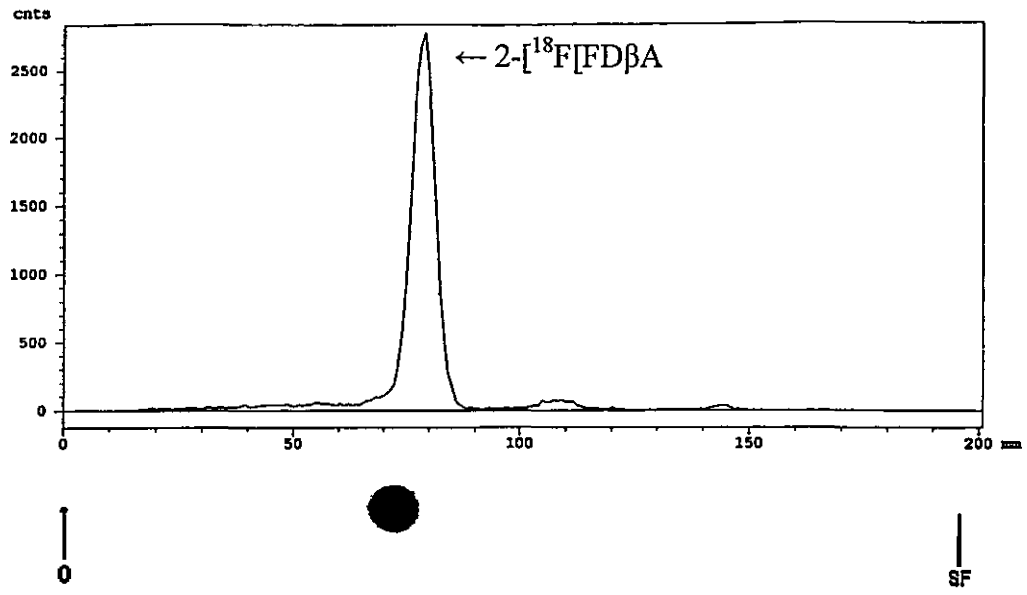
cnts
2500
2000
1500
1000
500
0
← 2-[^{18}F[FDβA
0
50
100
150
200 mm
0
SF

b)

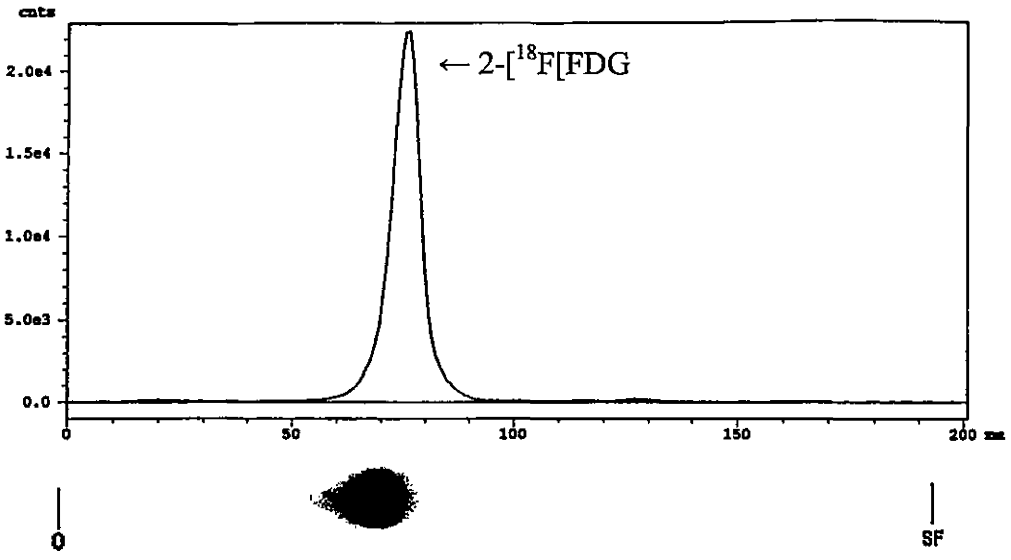
cnts
2.0e4
1.5e4
1.0e4
5.0e3
0.0
← 2-[^{18}F[FDG
0
50
100
150
200 mm
0
SF

Figure 4.2. Radio-HPLC chromatograms of (a) the products resulting from the electrophilic fluorination of TAG in aHF and (b) 2-[^{18}F]FDG.

a)

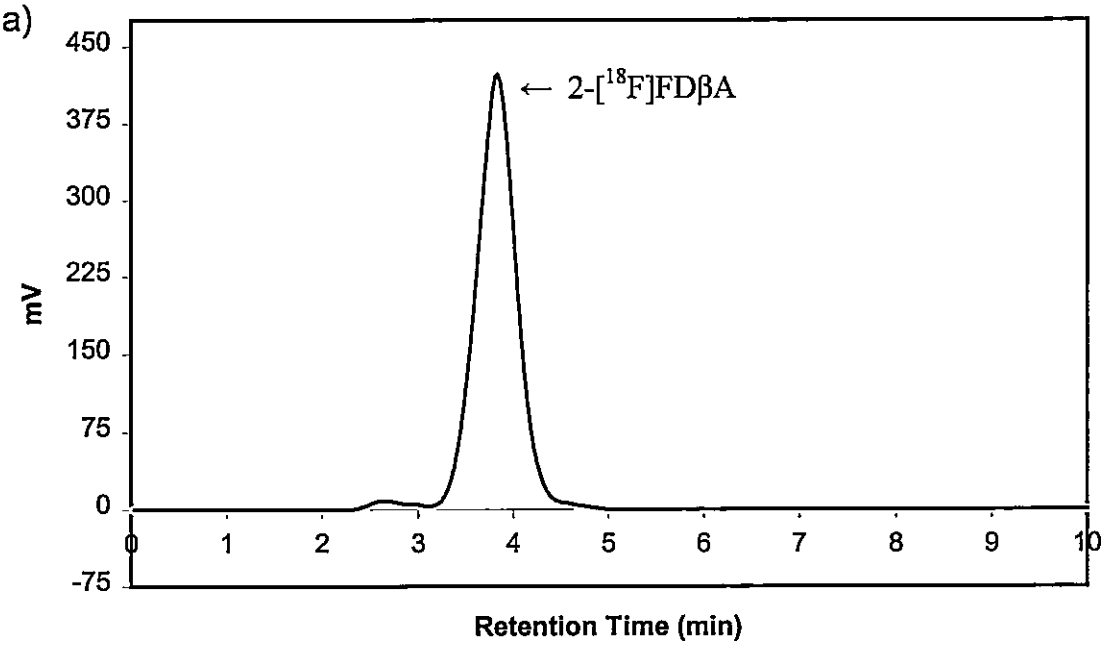
← 2-[18F]FDβA
450
375
300
225
150
75
0
-75
mV
0
1
2
3
4
5
6
7
8
9
10
Retention Time (min)

b)

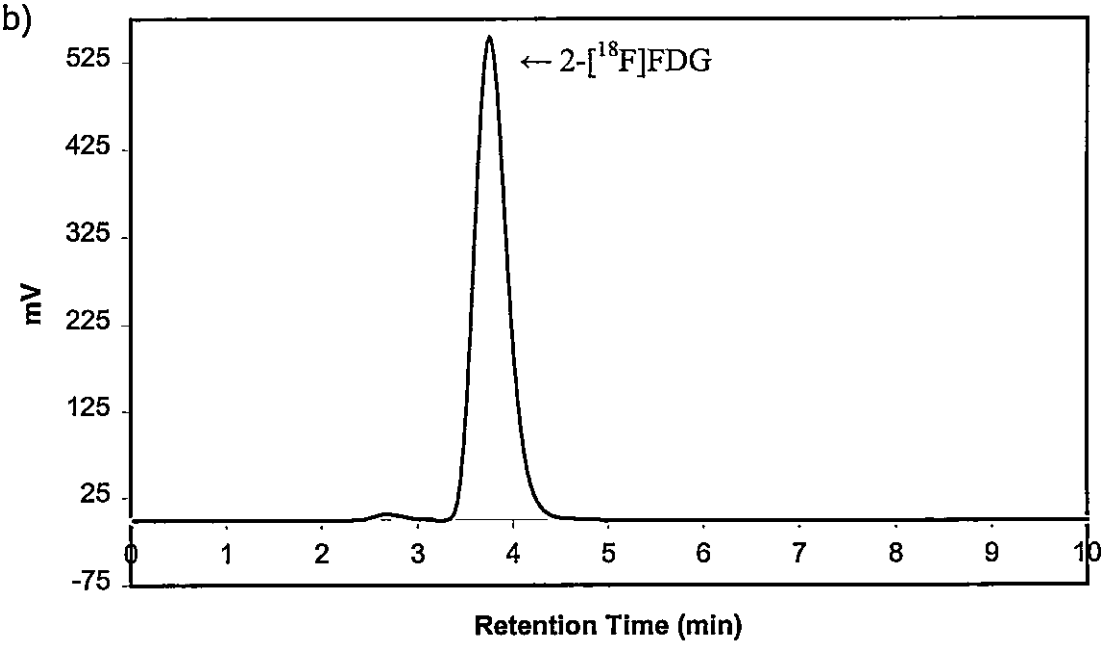
← 2-[18F]FDG
525
425
325
225
125
25
-75
mV
0
1
2
3
4
5
6
7
8
9
10
Retention Time (min)

workers showed, from a freshly prepared aHF solution of TAG, that the double bond of the corresponding 1,2-unsaturated 3,4-dioxolenium ion was initially intact at -70 °C. After a period of 24 h, the ^{1}H NMR spectrum showed that HF had added across the double bond of the dioxolenium ion in a Markovnikov fashion. The presence of a small amount of water hydrolyzed the dioxolenium ion and resulted in epimerization at C3.[93] In the present study, fluorinations were routinely carried out at -60 °C within 30 min following addition of aHF to TAG, thus avoiding significant HF addition to the double bond of the 1,2-unsaturated dioxolenium ion prior to fluorination.

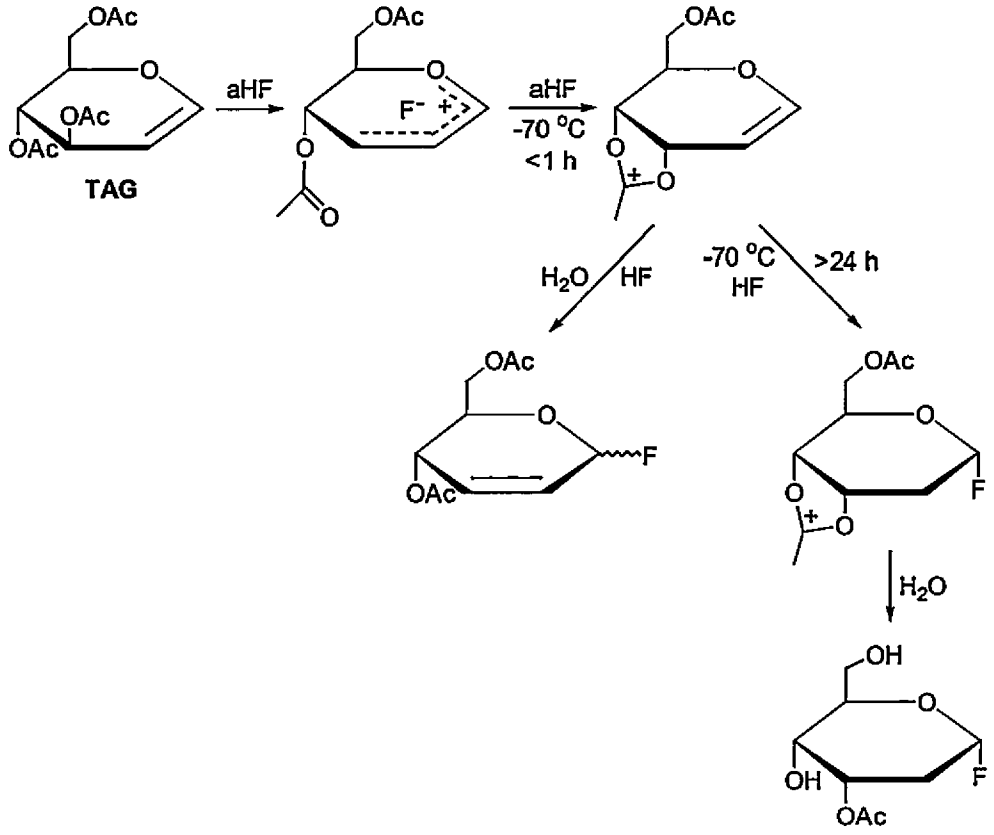

Scheme 4.2. Reaction of TAG with aHF.[93]

By incorporation of the existing synthetic route to 2-fluoro-2-deoxy sugars and the proposed synthetic route[93] that gives rise to the 1,2-unsaturated 3,4-dioxolenium ion and

its epimerization at C3, a possible reaction mechanism for the synthesis of 2-FDβA in the present work is arrived at (Scheme 4.3).

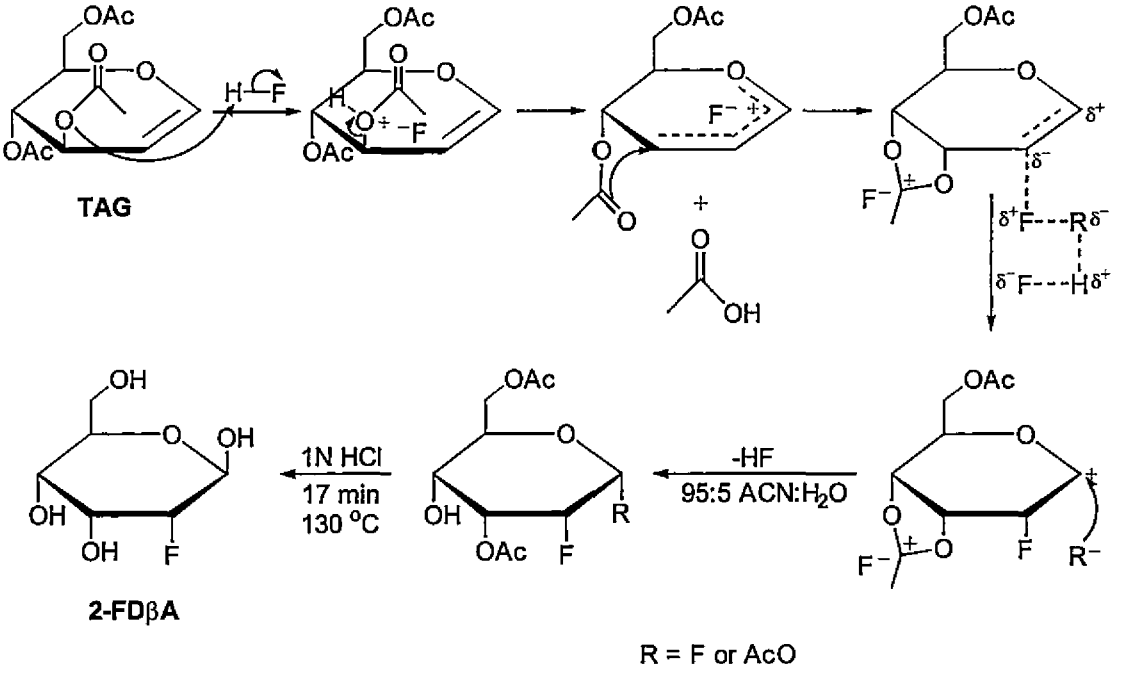

Scheme 4.3. A possible partial reaction mechanism for the synthesis of 2-FDβA by electrophilic fluorination of TAG in aHF.

In the last step of Scheme 4.3, the fluorine atom or the AcO group at C1 is readily replaced by a hydroxyl group upon hydrolysis. As a result, when $[^{18}F]F_2$ is used as the electrophilic fluorinating agent, ca. 50% of the ^{18}F radioactivity present in the difluoro intermediate will be lost upon hydrolysis, as is seen when the fluorinated intermediate resulting from the fluorination of TAG in $CFCl_3$ (Scheme 4.4) is hydrolyzed. The final product solution from Scheme 4.4 contains an approximately 2:1 mixture of 2-[^{18}F]FDG and 2-[^{18}F]FDM. The radiochemical data from this reaction (Table 4.1) shows that after hydrolysis, ca. 50% of the ^{18}F radioactivity present in the reaction intermediate (Table 4.1; Entry 6) immediately before hydrolysis is trapped on the ion retardation column and alumina Sep-Pak® (Table 4.1; Entry 9-11) that are used to purify the hydrolyzed products from ionic and inorganic impurities, whereas 44% of the ^{18}F

radioactivity was found in the final products (Table 4.1; Entry 12) and 8% remained in the hydrolysis vessel (Table 4.1; Entry 8).

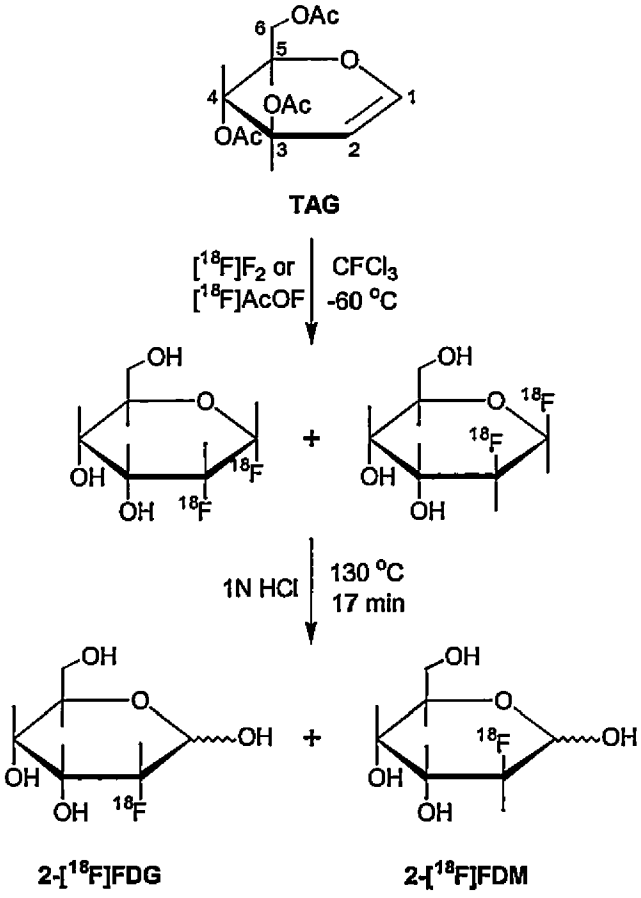

Scheme 4.4. Synthesis of 2-[^{18}F]FDG and 2-[^{18}F]FDM by electrophilic radiofluorination of TAG in $CFCl_3$.

It was, however, found that when fluorination was carried out in aHF, 9% of the ^{18}F radioactivity present in the reaction intermediate (Table 4.2; Entry 7) immediately before hydrolysis was trapped on the ion retardation column and alumina Sep-Pak® (Table 4.2; Entry 10-12) and 82% was found in the final products (Table 4.2; Entry 13). Therefore, the mechanism in Scheme 4.3 does not hold and it may be concluded that in aHF, fluorine does not undergo *syn* addition to the double bond. Instead, fluorination only occurs at C2 as a result of attack of C1 by the carbonyl oxygen of acetic acid. Because the bulky dioxolenium ion sterically hinders the bottom face of the double bond,

acetic acid preferably approaches C1 from the top face. Hence, fluorine adds to C2 from the bottom face. This mechanism accounts for the high regio- and stereoselectivity in te fluorination of TAG in aHF towards 2-fluoro-2-deoxy-D-allose. Scheme 4.5 shows a more plausible reaction mechanism for the synthesis of 2-FDβA.

Although the α/β anomeric equilibrium exists for every pyranoid sugar, the equilibrium for the D-*ribo*- and D-*allo*-pyranose series favors the β-D-pyranose form.[107,108] The exclusive existence of the β-configuration of 2-deoxy-2-(*R*)-fluoro-D-allose in the study is attributed to the dominance of the β-D-*allo*-pyranose form in the anomeric equilibrium as shown by absence of the α-anomer in the ^{1}H and ^{13}C NMR spectra.

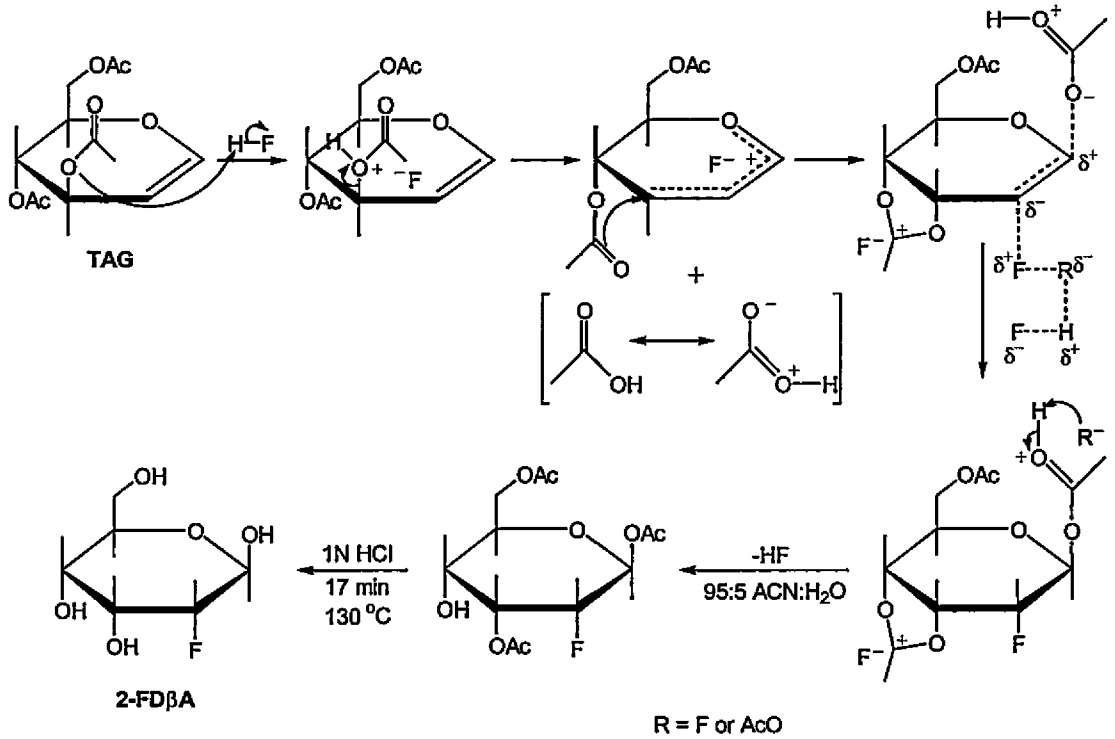

Scheme 4.5. A proposed partial reaction mechanism for the synthesis of 2-FDβA by electrophilic fluorination of TAG in aHF.

Table 4.1. Radiochemical Data from the Fluorination of TAG in $CFCl_3$ with $[^{18}F]F_2$

Entry	Sample	Actual Activity (mCi)	Time		Decay Factor	Decay-corrected Activity (mCi)	RCY w.r.t. $[^{18}F]F_2$ (%)
			Actual (hh:mm:ss)	Δt (min)			
1	NaOH trap	0.36	13:02:55	n/a	n/a	n/a	n/a
2	Reaction mixture in $CFCl_3$	177.80	13:04:20	0.00	1.0000	177.80	100.00
3	Empty reaction vessel after rinsing with 95:5 ACN:H_2O	0.27	13:08:30	4.17	0.9741	0.28	0.15
4	Silica Sep-Pak® and syringe	41.00	13:09:10	4.83	0.9700	42.27	23.77
5	Reaction intermediate after passing through silica Sep-Pak®	108.60	13:09:45	5.42	0.9664	112.37	63.20
6	Reaction intermediate after evaporation of 95:5 ACN:H_2O	98.00	13:20:35	16.25	0.9027	108.57	61.06
7	Crude product after hydrolysis	78.30	13:38:55	34.58	0.8042	97.37	54.76
8	Empty hydrolysis vessel	6.30	13:45:15	40.92	0.7727	8.15	4.59
9	Ion-retardation column	4.48	13:46:00	41.67	0.7691	5.83	3.28
10	Alumina Sep-Pak®	35.80	13:46:35	42.25	0.7663	46.72	26.28
11	C-18 Sep-Pak®	1.70	13:46:45	42.42	0.7655	2.22	1.25
12	Final product	33.80	13:47:30	43.17	0.7618	44.37	24.95

Table 4.2. Radiochemical Data from the Fluorination of TAG in aHF with $[^{18}F]F_2$

Entry	Sample	Actual Activity (mCi)	Time		Decay Factor	Decay-corrected Activity (mCi)	RCY w.r.t. $[^{18}F]F_2$ (%)
			Actual (hh:mm:ss)	Δt (min)			
1	NaOH trap	3.50	11:46:55	n/a	n/a	n/a	n/a
2	Reaction mixture in aHF	78.00	11:48:10	0.00	1.0000	78.00	100.00
3	Reaction vessel after pumping aHF off	39.80	12:10:35	22.42	0.8683	45.84	58.77
4	Empty reaction vessel after rinsing with 95:5 ACN:H_2O	0.50	12:16:30	28.33	0.8365	0.60	0.77
5	Silica Sep-Pak® and syringe	1.68	12:17:40	29.50	0.8304	2.02	2.59
6	Reaction intermediate after passing through silica Sep-Pak®	30.00	12:18:10	30.00	0.8278	36.24	46.46
7	Reaction intermediate after evaporation of 95:5 ACN:H_2O	25.00	12:32:30	44.33	0.7563	33.06	42.38
8	Crude product after hydrolysis	21.90	12:50:30	62.33	0.6752	32.44	41.58
9	Empty hydrolysis vessel	0.93	13:02:35	74.42	0.6257	1.48	1.90
10	Ion-retardation column	0.71	13:03:05	74.92	0.6237	1.14	1.46
11	Alumina Sep-Pak®	1.21	13:03:30	75.33	0.6221	1.95	2.49
12	C-18 Sep-Pak®	0.85	13:03:50	75.67	0.6208	1.37	1.76
13	Final product	16.70	13:04:10	76.00	0.6195	26.96	34.56

Table 4.3. Radiochemical Data from the Fluorination of TAG in aHF with [^{18}F]AcOF

Entry	Sample	Actual Activity (mCi)	Time		Decay Factor	Decay-corrected Activity (mCi)	RCY w.r.t. [^{18}F]F_2 (%)
			Actual (hh:mm:ss)	Δt (min)			
1	NaOH trap	2.40	14:41:20	n/a	n/a	n/a	n/a
2	Reaction mixture in aHF	50.30	14:43:10	0.00	1.0000	50.30	100
3	AcOF column	76.00	14:44:30	n/a	n/a	n/a	n/a
4	Reaction vessel after pumping aHF off	7.20	14:47:50	4.67	0.9710	7.41	14.74
5	Empty reaction vessel after rinsing with 95:5 ACN:H_2O	0.03	14:52:50	9.67	0.9409	0.03	0.06
6	Silica Sep-Pak® and syringe	0.15	14:51:55	8.75	0.9464	0.16	0.32
7	Reaction intermediate after passing through silica Sep-Pak®	6.30	14:52:20	9.17	0.9439	6.67	13.27
8	Reaction intermediate after evaporation of 95:5 ACN:H_2O	5.37	15:05:00	21.83	0.8715	6.16	12.25
9	Crude product after hydrolysis	4.86	15:23:55	40.75	0.7735	6.28	12.49
10	Empty hydrolysis vessel	0.10	15:32:15	49.08	0.7340	0.14	0.27
11	Ion-retardation column	0.12	15:33:00	49.83	0.7305	0.16	0.31
12	Alumina Sep-Pak®	0.20	15:33:50	50.67	0.7267	0.28	0.55
13	C-18 Sep-Pak®	0.11	15:34:30	51.33	0.7236	0.15	0.29
14	Final product	4.12	15:31:25	48.25	0.7378	5.58	11.10

4.2.4 Application of 2-[^{18}F]FDβA in PET Studies

Whole body imaging of normal rats by the use of a small animal imaging PET scanner showed differences between the biodistribution of 2-[^{18}F]FDG and 2-[^{18}F]FDβA (Figure 4.3.a) and b)). Whereas a significant amount of 2-[^{18}F]FDG was accumulated in the olfactory bulbs and the brain, 2-[^{18}F]FDβA showed no uptake in these organs. Furthermore, unlike 2-[^{18}F]FDG, 2-[^{18}F]FDβA was retained in the kidney. Additional animal studies were carried out using a Polynoma Middle T mouse model. Uptake of both 2-[^{18}F]FDG and 2-[^{18}F]FDβA were clearly visible in the tumours (Figure 4.4). The major difference between the two images was again that 2-[^{18}F]FDG was retained in the brain while no uptake of 2-[^{18}F]FDβA in the brain was observed.

4.3 Conclusion

Fluorine-18 labelled 2-FDβA has been synthesized for the first time by electrophilic fluorination of TAG in aHF with [^{18}F]F_2 and [^{18}F]AcOF with an overall decay-corrected RCY of 33 ±3% and 9 ±2%, respectively, with respect to [^{18}F]F_2. The radiochemical purity of the labelled compound was 96.3 ±3% and 91 ±8% as determined by radio-HPLC and radio-TLC, respectively. Preliminary *in vivo* studies showed that 2-[^{18}F]FDβA was likely to be a strong candidate for detection of breast tumour by PET. Additional *in vivo* studies are underway to further determine the potential application of 2-[^{18}F]FDβA in PET as a tracer for D-allose metabolism.

Figure 4.3. PET scans after administration of (a) 2-[^{18}F]FDG and (b) 2-[^{18}F]FDβA in normal rats.

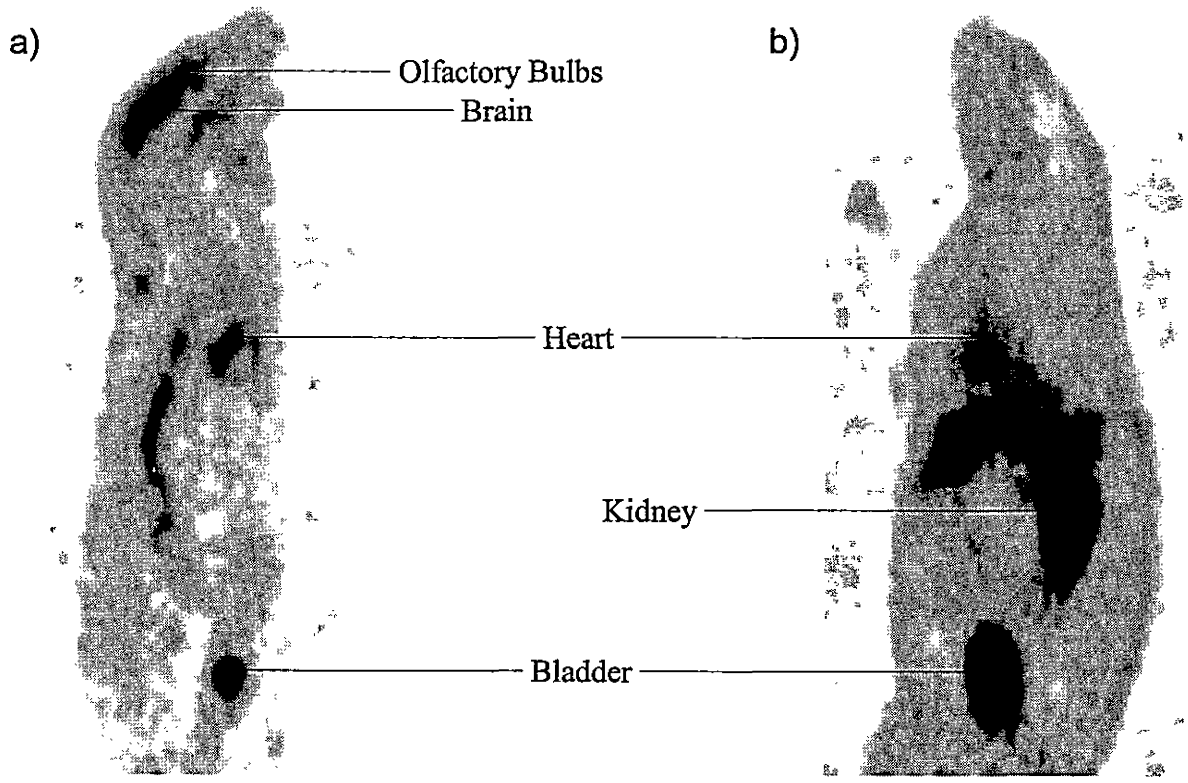
a)
Olfactory Bulbs
Brain
Heart
Bladder
b)
Kidney

Figure 4.4. PET scans after administration of (a) 2-[^{18}F]FDG and (b) 2-[^{18}F]FDβA in a Polynoma Middle T mouse model.

a)

b)

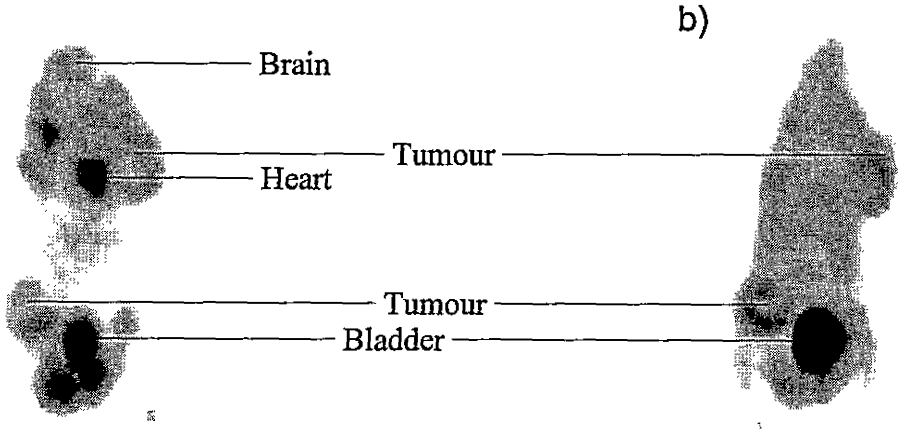

CHAPTER 5

SUMMARY AND DIRECTIONS FOR FUTURE RESEARCH

5.1 Summary

The present work employed direct fluorination techniques using electrophilic fluorine sources. Electrophilic fluorination of TAG in aHF resulted in the synthesis of 2-FDβA, which proved to be more rapid and efficient and less laborious than the existing synthesis reported by Johansson and Lindberg[84] in 1966. The present synthesis of 2-FDβA was also highly regio- and stereoselective, which is often not observed for direct fluorination reactions. A full characterization of 2-FDβA had not been reported prior to the present study and was accomplished by ^{1}H, ^{13}C and ^{19}F NMR spectroscopy and mass spectrometry.

The aforementioned synthetic route to 2-FDβA was applied to obtain the ^{18}F-labelled analogue, 2-[^{18}F]FDβA, for the first time. The overall decay-corrected RCYs were 33 ±3% and 9 ±2% with respect to [^{18}F]F_2 when [^{18}F]F_2 and [^{18}F]AcOF, respectively, were used as the electrophilic radiofluorinating agents. The RCY of 33 ±3% is the highest reported for direct electrophilic fluorinations of TAG using [^{18}F]F_2 in any other solvent. The radiochemical purities of 2-[^{18}F]FDβA were determined by radio-HPLC and radio-TLC to be 96 ±3% and 91 ±8%, respectively. Preliminary *in vivo* studies using normal rats showed significant differences between the uptake of 2-[^{18}F]FDβA and 2-[^{18}F]FDG in organs. Whereas 2-[^{18}F]FDβA showed no uptake in the olfactory bulbs and the brain, a significant amount of 2-[^{18}F]FDG was accumulated in these organs. Furthermore, unlike 2-[^{18}F]FDG, 2-[^{18}F]FDβA was retained in the kidney. Additional animal studies with a Polynoma Middle T mouse showed retention of 2-[^{18}F]FDβA in the tumour. The

^{18}F-labelling technique was also used as a mechanistic probe for the synthesis of 2-FDβA in the present study.

5.2 Directions for Future Research

The exploration of the mechanistic routes to 2-FDβA should be extended by studying the behaviour of TAG in aHF at different temperatures and/or over a given period of time by the use of variable temperature NMR spectroscopy. Such investigations will aid in determining at what point HF commences addition to the double bond of the 1,2-unsaturated 3,4-dioxolenium ion (see Chapter 4, Section 4.2.3). This will, in turn, determine whether or not the double bond of the dioxolenium ion was intact prior to fluorination in the present study.

The radiochemical purity of 2-[^{18}F]FDβA can be enhanced by developing an HPLC method to purify the compound from side products that result from the fluorination of TAG in aHF. This may help to isolate the compound, which is likely a fluorinated sugar, that gives rise to the unassigned "doublet of doublets" at -199.44 ppm in the ^{19}F NMR spectrum of the products (see Chapter 3, Figure 3.8) and allow its characterization. In addition, characterizing the by-products will help to understand the reaction mechanism better.

A more practical and reliable synthesis of 2-[^{18}F]fluoro-2-deoxy-D-allose by a no-carrier-added nucleophilic substitution method should be developed in order to increase both the RCY and the radiochemical purity of the compound. One possible synthetic approach is provided in Scheme 5.0 and is similar to the nucleophilic synthesis of 2-[^{18}F]FDG reported by Hamacher and co-workers.[109] The latter synthesis employs a regio- and stereospecific nucleophilic substitution of anhydrous $^{18}F^-$ for the triflate anion

leaving group in the precursor, 1,3,4,6-tetra-*O*-acetyl-2-*O*-trifluoromethane-sulfonyl-β-D-mannopyranose (mannose triflate), using 4,7,13,16,21,24-hexaoxa-1,10-diazabicyclo[8.8.8]hexacosane (2,2,2-crypt) as a phase transfer agent.

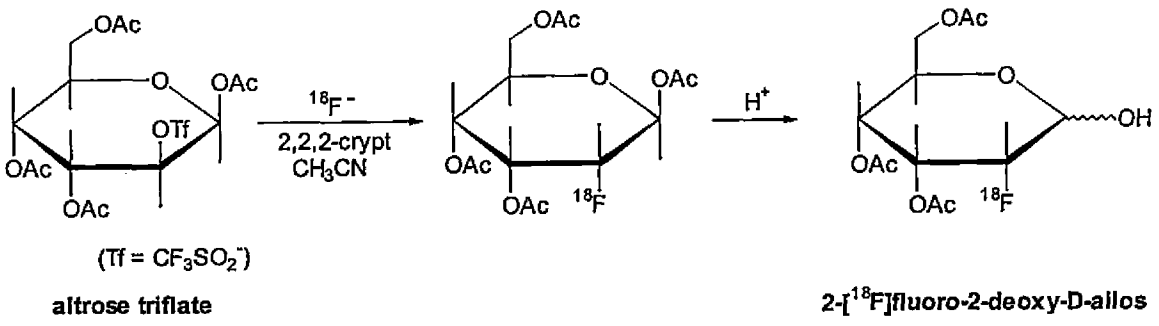

Scheme 5.0. A possible regio- and stereospecific nucleophilic synthesis of 2-[^{18}F]fluoro-D-allose.

Because the starting material in Scheme 5.0, altrose triflate (1,3,4,6-tetra-*O*-acetyl-2-*O*-trifluoromethane-sulfonyl-β-D-altropyranose), is not commercially available, it will be necessary to develop a reliable synthesis of this compound. One may be able to follow synthetic procedures that are similar to those for mannose triflate, the starting material in the 2-[^{18}F]FDG synthesis, that have been developed by Deferrari and co-workers,[110] Hamacher[111] and Barrio and co-workers.[112] This will entail selective acetylation of D-altrose to give 1,3,4,6-tetra-*O*-acetyl-2-*O*-trifluoromethane-sulfonyl-β-D-altropyranose, followed by triflation.

It is imperative that *in vivo* studies using 2-[^{18}F]FDβA be extended to establish its potential as a PET tracer. Animals possessing different types of tumour can be used in these studies. Both image and biodistribution data should be obtained from these studies and compared with those obtained using 2-[^{18}F]FDG.

REFERENCES

(1) Haszeldine, R.N.; Sharpe, A.G. *Fluorine and Its Compounds;* Methuen & Co. Ltd: London, 1951; p 1.

(2) Dobbin, L. *The Collected Papers of Carl Willhelm Scheele;* Kraus Reprint Co.: New York, NY, 1971; pp 3-16.

(3) Davy, H. *Phil. Trans.* **1813**, *103*, 263.

(4) Moissan, H. *Compt. Rend.* **1886**, *102*, 1543.

(5) Moissan, H. *Compt. Rend.* **1886**, *103*, 202.

(6) Moissan, H. *Compt. Rend.* **1886**, *103*, 256.

(7) Pauling, L. *The Nature of the Chemical Bond and the Structures of Molecules and Crystals: An Introduction to Modern Structural Chemistry;* 2nd Ed.; Cornell University Press: New York, NY, 1942; p 60.

(8) Wasastjerna, J.A. *Comment. Phys.-math. Helsingf.* **1923**, *1*, 1.

(9) Tewson, T. J. *Applications of Nuclear and Radiochemistry;* Pergamon Press: New York, NY, 1982; pp 163,164.

(10) Chambers, R.D. *Fluorine in Organic Chemistry;* Blackwell Publishing Ltd.: Oxford, 2004; pp 13,37.

(11) Schmitt, R.; von Gehren, H. *J. Prakt. Chem.* **1870**, *1*, 394.

(12) Lagow, R.J.; Margrave, J.L. *Prog. Inorg. Chem.* **1979**, *26*, 161.

(13) *CRC Handbook of Chemistry and Physics;* Lide, D.R., Ed.; 84th ed.; CRC Press: Boca Raton, 2003.

(14) Clark, J.H.; Wails, D.; Bastock, T.W. *Aromatic Fluorination;* CRC Press: Boca Raton, 1996; pp 1-17.

(15) Hutchinson, J.; Sandford, G. In *Top. Curr. Chem.* **1997**, *193*, 3.

(16) *Handbook of Radiopharmaceuticals: Radiochemistry and Application;* Welch, M.J.; Redvanly, C.S., Eds.; John Wiley & Sons Ltd.: Chichester, 2003; pp 42,43,249,198-200,

(17) Park, B.K.; Kitteringhan, N.B. *Drug Metab. Rev.* **1994**, *26*, 605.

(18) Ohno, A.; Shimizu, M.; Yamada, S. *Chem. Pharm. Bull.*, **2002**, *50*, 475.

(19) Satyamurthy, N.; Namavari, M.; Barrio, J.R. *Chemtech*, **1994**, 25.

(20) Lasne, M.-C.; Perrio, C.; Rouden, J.; Barré, L.; Roeda, D.; Dolle, F.; Crouzel, C. In

Top. Curr. Chem. **2002**, *222*, 203.

(21) Adloff, J. P.; Guillamumont, R. *Fundamentals of Radiochemistry;* CRC Press Inc.: Florida, 1993; pp 57-58, 79-80, 379,395.

(22) Chandra, R. *Nuclear Medicine Physics: The Basics;* 5th ed.; Lippincott Williams & Wilkins: Baltimore, 1998; pp 8-13, 38-41.

(23) Saha, G. *Fundamentals of Nuclear Pharmacy;* 4th ed.; Springer: New York, 1998; pp 12,14,80.

(24) *Fundamentals of Nuclear Medicine;* Alazraki, N.P.; Mishkin, F.S., Eds.; The Society of Nuclear Medicine Inc.: New York, 1984; p 174.

(25) Chandra, R. *Introductory Physics of Nuclear Medicine;* 2nd ed.; Lea & Febiger: Philadelphia, 1982; p 57.

(26) Phelps, M. *J. Nucl. Med.*, **2000**, *41*, 661.

(27) *PET for Drug Development and Evaluation;* Comar, D., Ed.; Developments in Nuclear Medicine, v. 26; Kluwer Academic Publishers: London, 1995; p 187.

(28) Syrota, A.; Jehenson, P. *Eur. J. Nucl. Med.* **1991**, *18*, 897.

(29) Ritter, S.K. *Chem. Eng. News* **1999**, *77*, 30.

(30) Kearfott, K.J.; Votaw, J.R. *Chemists' Views of Imaging Centers;* Proceedings of an American Chemical Society Symposium on Chemists' Views of Imaging Centers, Chicago, Aug. 22-27, 1993; Plenum Press: New York, 1995; p 3.

(31) Wilson, M.A.; Hammers, R.J. *Textbook of Nuclear Medicine;* Wilson, M.A., Ed.; Lippincott-Raven: Philadelphia, 1998; pp 385-390.

(32) Chirakal, R. Ph.D thesis, McMaster University, Hamilton, ON, 1991; pp 12,15-19.

(33) Vasdev, N. Ph.D thesis, McMaster University, Hamilton, ON, 2003; pp 4,10-12.

(34) Matsson, O.; Persson, J.; Axelsson, B.S.; Langström, B. *J. Am. Chem. Soc.* **1993**, *115*, 5288.

(35) Winfield, J.M. *J. Fluorine Chem.* **1980**, *16*, 1.

(36) Stöcklin, G. L. *Eur. J. Nucl. Med.*, **1998**, *25*, 1612.

(37) Nickles, R.J.; Gatley, S.J.; Votaw, J.R.; Kornguth, M.L. *Appl. Radiat. Isot.* **1986**, *37*, 649.

(38) Ruth, T.J.; Wolf, A.P. *Radiochimica Acta* **1979**, *26*, 21.

(39) Thomas, C.C., Jr.; Sondel, J.A.; Kerns, R.C. *Int. J. Appl.Radiat. Isot.* **1965**, *16*, 71.

(40) Nozaki, T.; Tanaka, Y.; Shimamura, A.; Karasawa, T. *Int. J. Appl.Radiat. Isot.* **1968**, *19*, 27.

(41) Nozaki, T.; Iwamoto, M.; Ido, T. *Int. J. Appl.Radiat. Isot.* **1974**, *25*, 393.

(42) Clark, J.C; Sivester, D.J. *Int. J. Appl.Radiat. Isot.* **1966**, *17*, 151.

(43) Fitschem, J.; Beckmann, R.; Holm, U.; Neuert, H. *Int. J. Appl.Radiat. Isot.* **1977**, *28*, 781.

(44) Bishop, A.; Satyamurthy, N.; Bida, G.; Phelps, M.; Bario, J.R. *Nucl. Med. Biol.* **1996**, *23*, 385.

(45) Nickles, R.J.; Daube, M.E.; Ruth, T.J. *Int. J. Appl.Radiat. Isot.* **1984**, *35*, 117.

(46) Firouzbahkt, M.L.; Schlyer, D.J.; Gatley, S.J.; Wolf, A.P. *J. Nucl. Med.* **1993**, *34*, 69P.

(47) Hughey, B.J.; Shefer, R.E.; Klinkowstein, R.E.; Welch, M.J.; Dence, C.S.; Livni, E. *J. Nucl. Med.* **1992**, *33*, 932.

(48) Kilbourn, M.R.; Jerabek, P.A.; Welch, M.J. *Int. J. Appl.Radiat. Isot.* **1985**, *36*, 327.

(49) Leonhardt, W. *Kernenergie* **1963**, *6*, 45.

(50) Ruth, T.J. *Int. J. Appl.Radiat. Isot.* **1985**, *36*, 107.

(51) Casella, V.; Ido, T.; Wolf, A.P.; Fowler, J.S.; MacGregor, R.R.; Ruth, T.J. *J. Nucl. Med.* **1980**, *21*, 750.

(52) Blessing, G.; Coenen, H.H.; Franken, K.; Qaim, S.M. *Int. J. Appl.Radiat. Isot.* **1986**, *37*, 1135.

(53) Crouzel, C.; Comar, D. *Int. J. Appl.Radiat. Isot.* **1978**, *29*, 407.

(54) Backhausen, H.; Stöcklin, G.; Weinreich, R. *Radiochimica Acta* **1981**, *29*, 1.

(55) Chirakal, R; Adam, R.M.; Firnau, G.; Schrobilgen, G. J.; Coates, G.; Garnett, E.S. *Nucl. Med. Biol.* **1995**, *22*, 111.

(56) Barton, D.H.R.; Godhino, L.S.; Hesse, R.H.; Pechet, M.M. *J. Chem. Soc., Chem. Commun.* **1968**, 804.

(57) Barton, D.H.R.; Ganguly, A.K.; Hesse, R.H.; Loo, S.N.; Pechet, M.M. *J. Chem. Soc., Chem. Commun.* **1969**, 806.

(58) Fukuhara, N.; Bigelow, L.A. *J. Am. Chem. Soc.* **1941**, *63*, 788.

(59) Fukuhara, N.; Bigelow, L.A. *J. Am. Chem. Soc.* **1941**, *63*, 2792.

(60) Chambers, R.D.; Skinner, C. J.; Hutchinson, J.; Thomson, J. *J. Chem. Soc., Perkin Trans. 1*, **1996**, 605.

(61) Moillet, J.S. *J. Fluorine Chem.*, **2001**, *109*, 13.

(62) Rozen, S.; Lerman, O.; Kol, M. *J. Chem. Soc., Chem. Commun* **1981**, 443.

(63) Appleman, E.H.; Mendelsohn, M.H.; Kim, H. *J. Am. Chem. Soc.* **1985**, *107*, 6515.

(64) Rozen, S. *Chem. Rev.* **1996**, *96*, 1717.

(65) Shiue, C.-Y.; Salvadori, P.A.; Wolf, A.P. *J. Nucl. Med.* **1982**, *23*, 899.

(66) Jewett, D.M.; Potocki, J.F.; Ehrenkaufer, R.E. *J. Fluorine Chem.* **1984**, *24*, 477.

(67) Chirakal, R.; Firnau, G.; Garnett, E.S. *Appl. Radiat. Isot.* **1988**, *39*, 1099.

(68) Smart, B.E. *J. Fluorine Chem.*, **2001**, *109*, 3.

(69) Kirk, K.L. *J. Fluorine Chem.*, **1995**, *72*, 261.

(70) Kirk, K.L. *J. Med. Chem.*, **1986**, *29*, 1982.

(71) Chirakal, R.; Vasdev, N.; Asselin, M.-C.; Schrobilgen, G. J.; Nahmias, C. *J. Fluorine Chem.*, **2002**, *115*, 33.

(72) Chirakal, R.; Vasdev, N.; Schrobilgen, G. J.; Nahmias, C. *J. Fluorine Chem.*, **1999**, *99*, 87.

(73) Vasdev, N.; Chirakal, R.; Schrobilgen, G. J.; Nahmias, C. *J. Fluorine Chem.*, **2001**, *111*, 17.

(74) Chirakal, R; Schrobilgen, G. J.; Firnau, G.; Garnett, E.S. *Appl. Radiat. Isot.*, **1991**, *42*, 113.

(75) Chirakal, R.; Firnau, G.; Garnett, E.S. *J. Nucl. Med.*, **1986**, *27*, 417.

(76) Chirakal, R.; Brown, K.L.; Firnau, G.; Garnett, E.S.; Hughes, D.W.; Sayer, B.G.; Smith, R.W. *J. Fluorine Chem.*; **1987**, *37*, 267.

(77) Reinhardt, C. F.; Hume, W. G.; Linch, A. L.; Wetherhold, J. M. *J. Chem. Ed.*, **1969**, *46*, A171.

(78) Segal, E. B. *Chem. Health Saf.*, **2000**, *7*, 18.

(79) Peters, D.; Miethchen, R. J. *J. Fluorine Chem.*, **1996**, *79*, 161.

(80) Gribble, G. W. *Chemosphere* **2003**, *52*, 289.

(81) Thomas, S.O.; Singleton, V.L.; Lowery, J.A.; Sharpe, R.W.; Preuss, L.M.; Porter,

J.N.; Mowat, J.H.; Bohonos, N. *Antibiotics Ann.* **1956**, 716.

(82) Morton, G.O.; Lancaster, J.E.; Van Lear, G.E.; Fulmor, W.; Meyer, W.E. *J. Am. Chem. Soc.* **1969**, *91*, 1535.

(83) Miethchen, R. *J. Fluorine Chem.*, **2004**, *125*, 895.

(84) Johansson, I.; Lindberg, B. *Carbohydr. Res.*, **1966**, *1*, 467.

(85) Buethium-Baumann, B.; Hamacher, K.; Oberdorfer, F.; Steinbach, *J. Carbohydr. Res.* **2000**, *327*, 107.

(86) Hossain, M.A.; Izuishi, K; Tokuda, M.; Izumori, K; Maeta, H. *J. Hepatobiliary Pancreat. Surg.* **2004**, *11*, 181.

(87) Arnold, E.C.; Silady, P.J. U.S. Patent 5,620,960,1997.

(88) Taylor, S.D.; Christopher, C.K.; Hum, G. *Tetrahedron* **1999**, *55*, 12431.

(89) Tsuchiya, T. *Adv. Carbohydr. Chem. Biochem.* **1990**, *48*, 91.

(90) Adamson, J; Foster, A.B.; Hall, L.D.; Hesse, R.H. *J. Chem. Soc., Chem. Commun.* **1969**, 309.

(91) Adamson, J; Foster, A.B.; Hall, L.D.; Johnson, R.N.; Hesse, R.H. *Carbohydr. Res.* **1970**, *15*, 351.

(92) Lundt, I.; Pedersen, C. *Acta Chem. Scand.* **1966**, *20*, 1369.

(93) Lundt, I.; Pedersen, C. *Acta Chem. Scand.* **1970**, *24*, 240.

(94) Lundt, I.; Pedersen, C. *Acta Chem. Scand.* **1971**, *25*, 2749.

(95) Ido, T.; Wan, C.-N.; Fowler, J.S., Wolf, A.P. *J. Org. Chem.* **1977**, *42*, 2341.

(96) Adam, M.J. *J. Chem. Soc., Chem. Commun.* **1982**, 730.

(97) Adam, M.J.; Pate, B.D.; Nesser, J.-R.; Hall, L.D. *Carbohydr. Res.* **1983**, *124*, 215.

(98) Bida, T. G.; Satyamurthy, N.; Barrio, J. R. *J. Nucl. Med.*, **1984**, *25*, 1327.

(99) Michalik, M.; Hein, M.; Frank, M. *Carbohydr. Res.*, **2000**, *327*, 185.

(100) Sigma-Aldrich product information webpage for β-D-allose; http://www.sigmaaldrich.com/spectra/fnmr/FNMR005499.PDF

(101) Ido, T.; Wan, C.-N.; Casella, V.; Fowler, J.S.; Wolf, A.P. *J. Label. Comp. Radiopharm.* **1978**, *14*, 175.

(102) Van Rijn, C.J.S.; Herscheid, J.D.M.; Visser, G.W.M.; Hoekstra, A. *Int. J. Appl. Radiat. Isot.* **1985**, *36*, 111.

(103) Ehrenkaufer, R.W.; Potocki, J.F.; Jewett, M. *J. Nucl, Med.* **1984**, *25*, 333.

(104) Fukuda, H; Takahashi, J.; Fujiwara, T.; Yamaguchi, K.; Abe, Y.; Kubota, K.; Sato, T.; Miyazawa, H.; Hatazawa, J.; Tada, M; *J. Nucl. Med.* **1993**, *34*, 780.

(105) Ishiwata, K; Yamaguchi, K.; Kameyama, M.; Fukuda, H.; Tada, M.; Matsuzawa, T.; Muraishi, K.; Itoh, J.; Kawashima, K.; Takahashi, T. *Int. J. Radiat. Appl. Instrum. B* **1989**, *16*, 247.

(106) Pengles, A.A. *Adv. Carbohydr. Chem. Biochem.* **1981**, *38*, 195.

(107) Lemieux, R.U. In *Molecular Rearrangements* Part 2, de Mayo, P., Ed.; Wiley-Interscience: New York, 1964; pp 735-743.

(108) Okumura, H.; Azuma, I. *Carbohydr. Res.* **1983**, *117*, 298.

(109) Hamacher, K.; Coenen, H.H.; Stöcklin, G.L *J. Nucl. Med.*, **1986**, *27*, 235.

(110) Deferrari, J.O.; Gros, E.G.; Mastronardi, I.O. *Carbohydr. Res.* **1967**, *4*, 432.

(111) Hamacher, K. *Carbohydr. Res.* **1984**, *128*, 291.

(112) Toyokuni, T.; Kumar, J.S.D.; Gunawan, P.; Basarah, E.S.; Liu, J.; Barrio, J.R.; Satyamurthy, N. *Mol. Imaging Biol.* **2004**, *6*, 324.